A Cross-Border Dynamic Land Use–Transport Model: Integrating Housing and Commuting in Luxembourg

Negar Rezvany [*] Tim Hillel [†] Michel Bierlaire [*]

August 2025

Report TRANSP-OR 250826
Transport and Mobility Laboratory
School of Architecture, Civil and Environmental Engineering
Ecole Polytechnique Fédérale de Lausanne
transp-or.epfl.ch

[*]École Polytechnique Fédérale de Lausanne (EPFL), School of Architecture, Civil and Environmental Engineering (ENAC), Transport and Mobility Laboratory, Switzerland, {negar.rezvany,michel.bierlaire}@epfl.ch

[†]University College London (UCL), Department of Civil, Environmental and Geomatic Engineering (CEGE), United Kingdom, {tim.hillel@ucl.ac.uk}

Abstract

This study presents a system dynamics framework that integrates transport and land use components internally, explicitly capturing their interrelations and model their evolution over time. The model operates at a discrete zonal scale with sub-annual time steps, enabling the representation of temporal lags at differing process speeds. A case study at a cross-national scale demonstrates the model's ability to capture interregional dynamics, including commuting flows that span administrative borders —essential in regions where labour markets and infrastructure extend beyond a single country. The framework incorporates endogenous feedbacks that drives the system behaviour, while remaining computationally efficient, thus enabling planners and policymakers to assess the aggregate effects of short- to long-term urban and transport strategies in a timely manner. Applied to the Greater Region of Luxembourg, the model reproduces observed dynamics and explores policy scenarios. Results show that infrastructure investments in isolation provide only temporary relief, emphasising the need for integrated, forward-looking housing and transport strategies.

Keywords: Decision Support tool; Dynamic modelling; System thinking; Housing location; Transport economics and policy.

1 Introduction

1.1 Motivation

Think of a territory where people are living in, whether urban or rural. Within such a context, a range of choices exists across (i) different time horizons such as short-term, mid-term, and long-term, and (ii) different levels of authority, from household and individual decisions to those of public authorities. Thus, there are various decisions made at different temporal, spatial, and hierarchical levels. Figure 1 presents example choices and decisions at different temporal and hierarchical levels together with their interactions.

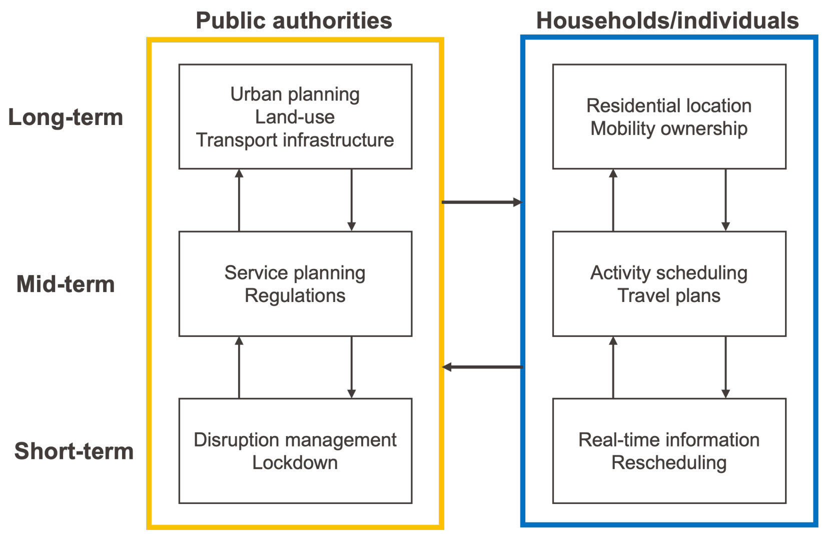

Figure 1: Choices and decisions in urban/rural context

Territories face challenges stemming from the interplay of transport and land use developments such as congestion, accessibility issues, increasing housing prices, housing shortage, relocation of residents, and migration. Transport and land use planning are highly interdependent, involving complex two-way causality; households and firms adapt their location decisions to the transport opportunities and accessibility -the ease of reaching jobs and services via the transport network- while those collective location patterns in turn reshape travel demand and network performance over time. For example transport investments change accessibility, accessibility changes location attractiveness, which alters land use, and this new land use pattern feeds back into transport demand and performance. Thus, for a structured urban decision-making process, we need a comprehensive model accounting for these spatial and temporal interrelations over time, enabling decision-makers to implement effective strategies towards defined goals.

The interactions between transport and land use are not effectively captured in conventional transport planning models, as land use is typically assumed to be constant and treated exogenously. Coordinating transport and land use planning is essential for informed and structured decision-making (Kaufmann and Jemelin, 2003). One approach to combine transport and land use sub-models is Land-Use Transport Interaction (LUTI) models (Wegener, 2021; Acheampong and Silva, 2015; Black, 2018; Bierlaire et al., 2015; Waddell, 2014). These models capture the connection between land use and transport by linking a location choice model for households or firms with a transport model of travel demand and network performance. They are used to assess the impact of given transport and land use policies, such as infrastructure expansion, new housing developments, or changes in public transport services and fares. They also serve to analyse broader socio-demographic trends (e.g., population growth, migration) and economic scenarios (e.g., economic growth/decline).

Land use and transport are parts of a dynamic system, evolving at different time scales: travel behaviour can adjust within days to months in response to congestion or cost changes, whereas land use evolves more slowly due to their considerable inertia, as they are tied to physical structures. This mismatch dynamic creates temporal asynchronies, with some urban processes responding sooner and others with a lag. Moreover, transport policies can have lasting long-term impacts on urban dynamics. For example, road pricing or transit expansions may affect congestion in short run, but also shift the spatial distribution of housing and employment in long term.

In static LUTI models, the link between the future projections and current conditions is neglected, as the trajectory toward future states is unspecified. Conventional LUTI models, similar to traditional transport modelling, follow the notion of equilibrium, assuming that urban systems are always in a state of stationary equilibrium. However, this assumption is unrealistic, as urban systems may never reach a long-term stationary equilibrium (Simmonds et al., 2013). The appeal of equilibrium lies in its analytical elegance, allowing for straightforward comparisons. However, it overlooks the inherent inertia of urban systems, which tend to evolve only gradually over many years. Instead, their co-evolution should be captured, moving beyond stationary equilibria to transitory equilibrium to reflect behavioural dynamics, market fluctuations, and policy responsiveness. The time horizon of urban planning extends into the long term, making it essential to explicitly recognise that urban systems are continuously evolving. The supply and demand are in constant motion, adjusting gradually over time. For example, increasing travel demand without corresponding infrastructure expansion leads to congestion and shifts in demand, while uneven residential demand drives rental price shifts and residential relocation. These changes often occur with time delays, reflecting the feedback-driven nature of urban systems, which rarely function in stationary equilibrium.

Moreover, aggregate system behaviour, critical for strategic decision-making, is often overlooked. To evaluate the long-term effects of multiple competing strategies, understanding the macroscopic dynamics of the urban system is essential. For strategic planning, factors such as data availability, low implementation cost, and short run times are often more valuable than highly detailed disaggregate precision. Acheampong and Silva (2015) argues that, in addition to the considerable demand for high-quality data, a key challenge of disaggregation is the long execution time required to run disaggregate models, which makes it difficult to evaluate the large number of scenarios needed for developing integrated strategies or policy packages. Current studies predominantly focus only on city-wide or nation-wide cases, overlooking cross-national spatial dimensions such as cross-border commuting and immigration. This is important especially for small countries with high economic growth and wages, where the cross-border commuters from neighbouring countries represent a substantial share of the workforce and daily commutes. Most existing strategic models use yearly timesteps, which fail to capture the shorter time lags of processes operating on monthly or daily scales. As a general guideline, Forrester (1970) recommends that the timestep should not exceed half the duration of the shortest time lag in the system. Furthermore, many models couple transport and land use components externally, rather than integrating them endogenously within a unified framework, which creates the additional challenge of ensuring consistent information exchange between sub-models.

Addressing these issues involves several challenges: (i) Explicitly modelling the dynamics between land use and transport systems is complex, as changes occur at different speeds—ranging from fast (e.g., transport users), to medium (e.g., residential location choices), to slow (e.g., infrastructure and land use developments). (ii) Each urban process has its own reaction speed, making it essential to account for their specific time lags. (iii) Striking a balance between sufficient accuracy to support data-driven planning, and computational efficiency presents an additional challenge (Kii et al., 2019). These limitations and challenges highlight an opportunity to advance the state of practice by endogenously integrating residential location and transportation within a single model, at a cross-national spatial scale, and using sub-annual timesteps to effectively capture processes with varying reaction speeds. Addressing this gap allows for the development of an efficient decision-support tool for evaluating potential policy interventions at a cross-national level with zonal spatial resolution.

1.2 Goals and objectives

In this manuscript, we develop a computationally quick dynamic model for transportation and land use over a time horizon of multiple years. The model's timestep is days so the time delays and reaction speeds of different processes can be effectively captured. We integrate transport and land use models within a unique framework, modelling the pathway of the transport and land use systems over time, explicitly accounting for their interactions. On the land use side, this study focuses on residential location choices and treats workplace as exogenously given in the model. The framework is developed at a cross-national spatial dimension, with spatial granularity of discrete zonal level to capture the transport and land use dynamics between different zones of a region through time. Our approach is based on the principles of System Dynamics (Sterman, 2000; Forrester, 1961), as a well-suited approach for complex systems that changes over time, due to their ability to model feedback, delays, and dynamic adaptation.

The focus of our study is the case of Luxembourg; a small country with exceptionally high levels of cross-border commuting. As of 2014, approximately 40% of Luxembourg's labour force consisted of cross-border workers residing in neighbouring countries (France, Belgium, and Germany) (Walczak and Mathae, 2018). This unique context requires any LUTI model to account for interactions that extend beyond national borders, as both housing markets and transport networks span multiple jurisdictions. Most existing models focus on a single metropolitan area, overlooking flows and interactions across administrative borders. Our model explicitly represents Luxembourg's internal cantons along with adjacent cross-border regions, capturing the dynamic feedback between domestic development and the external commuting hinterland. For instance, increasing housing demand within Luxembourg, combined with limited housing supply, may lead more households to settle in neighbouring regions —thereby intensifying cross-border traffic. This extended application addresses a limitation in typical LUTI cases, which rarely consider multi-country systems or the policy coordination issues they entail.

The remainder of this manuscript is structured as follows. We give a review of the literature in Section 2. The contributions of this work are summarised next in Section 3. The integrated framework is explained in Section 4. An illustrative example for the case of Luxembourg is presented in Section 5 to showcase the capabilities of the proposed framework. The concluding remarks and opportunities for future research are discussed in Section 6.

2 Relevant literature

In classical transport modelling practice, land use inputs -such as population and employment distributions- are typically treated exogenously. Most conventional travel demand models assume a predetermined land use scenario that does not change in response to transportation improvements (Johansen et al., 2015). In fact, transport project evaluations often hold land use constant between the base case and project case, meaning any shifts in where people live or work are ignored when forecasting. This simplifying assumption makes modelling more straightforward, but it fails to capture the two-way feedback between transport and land developments. As a result, analyses based on exogenous land use can misestimate long-term impacts, since they exclude the potential land use changes spurred by improved accessibility (Le et al., 2023).

LUTI models formalise the linkage between where people live (land use) and how they travel (transport), by combining a land use component (often a model of household or firm location choice) with a transport component (modelling travel demand and network performance). The first operational model to implement a land use transport feedback cycle was based on analogies to physics, Lowry's Model of Metropolis (Lowry, 1964), a spatial interaction model, allocating population and employment across zones based on accessibility in a gravity model. Though static in nature, the Lowry's model provided a template for how transport accessibility can drive land use patterns in an aggregate model. This work inspired a wave of increasingly complex models in the 1970s and 1980s (Putman, 1983; Mackett, 1983; Goldner, 1971; Echeñique et al., 1969). These pioneering efforts established the foundation for treating land use and transport as a unified, interacting system rather than as isolated components.

Multiple approaches exist to model transport within land use models. LUTI models can be broadly classified along two key dimensions: (i) the treatment of time, and (ii) the level of aggregation. In terms of time dynamics, models are either (i) static; focusing on a single time point without explicitly considering how the system evolves, or (ii) dynamic; capturing the development path over time and allow for feedback effects and temporal adjustments. In terms of aggregation, models range from (i) aggregates; working with zonal averages or market-level quantities, to (ii) disaggregate; simulating individual agents such as households or firms. Recent reviews emphasise this classification (Moeckel et al., 2018; Sivakumar, 2007; Timmermans, 2006). We highlight foundational and recent literature for major categories of LUTI modelling approaches.

Discrete choice models based on random utility theory originating from micro-economics (Haque et al., 2019; Yang et al., 2013; Lee and Waddell, 2010; Vega and Reynolds-Feighan, 2009; Mokhtarian and Cao, 2008; Martínez and Henríquez, 2007; Bhat and Guo, 2007; Ben-Akiva and Bowman, 1998; Lerman, 1976; Domencich and McFadden, 1975; McFadden, 1974) and mathematical programming models (Bravo et al., 2010; Pinjari et al., 2009; Alonso, 1964; White, 1988) represent a class of disaggregate static models. These models maximise household utility while describing the interaction between transportation and activity location. By incorporating detailed location characteristics and individual decision-making behaviour through a wide range of indicators, random utility models provide valuable insights but remain too simplistic to fully capture the complex interplay between transportation and land use; in particular, they do not explicitly model the feedback loop between urban transport and residential location choices. There are also examples of other modelling approaches, such as the application of bi-level optimisation to capture the relationship between traffic cost impedance and location attractiveness (Chang and Mackett, 2006). However, finding an optimal solution to a bi-level programming problem is often challenging in practice. Although disaggregate static models capture heterogeneity, they do not account for temporal evolution and are therefore more suitable for assessing immediate impacts.

In contrast to disaggregate models that focus on individual agents and their choices, aggregate models analyse the behaviour of groups or zones as a whole. They seek to represent the equilibrium of markets (housing, labour, transport) at a macroscopic level. Spatial computable general equilibrium (SCGE) models are a prime example of aggregate static frameworks, borrowing methods from economic general equilibrium theory (Tscharaktschiew and Hirte, 2012; Anas and Liu, 2007; Anas, 1994). These models typically solve for a simultaneous equilibrium in land use and transport given supply/demand relationships, but often for a single time period, which can then be updated exogenously or in steps. SCGE models are example aggregate static models, bridging between spatial economics and transport modelling by emphasising market-level outcomes rather than individual behaviour. Earlier aggregate models, such as MEPLAN (Echenique et al., 1990; Echeñique et al., 1969) and TRANSUS (de la Barra, 1989) , while not full computational general equilibrium in the modern sense, used spatial input-output and equilibrium concepts to integrate land use and transport. They paved the way for later SCGE models by showing that one can link economic activities, land use, and transport in an equilibrium-consistent manner.

Aggregate static models are powerful for economic appraisal and theoretical insight, though ignore dynamic and temporal co-evolution of urban land use and transport networks. The common feature of these models is their lack of memory; they allocate activities afresh in each period without reference to past states. Spatial interaction models do not account for time and often conflate processes with different temporal dynamics —linking slow, inert location changes with fast, flexible travel behaviour without considering the lagged effect of accessibility in location choice. Static equilibrium models assume that interdependent variables -such as prices, supply, and demand— adjust instantaneously to reach equilibrium, without accounting for the sequence of events or path dependence. These models abstract away from time and do not represent temporal dynamics or chronological progression. By forecasting static outcomes, they often omit slow processes and inertia effects. As a result, they risk mis-estimating responses to change, with no assurance that over- and under-statements will balance out.

Microsimulation models extend disaggregate approaches into the dynamic domain. UrbanSim (Waddell, 2002) coupled with a transport model such as MATSIM (Axhausen et al., 2016), ILUTE (Salvini and Miller, 2005), and ILUMASS (Moeckel et al., 2007) demonstrate how microsimulation can incorporate both random utility models and rule-based processes to capture urban markets (housing, labour, transport) in a unified way, are example microsimulation models. de Palma et al. (2005) develop a modelling framework that couples UrbanSim with a dynamic traffic assignment model, explicitly capturing two forms of endogeneity in residential location choices: the interdependence between residential location and rent prices, and the interdependence between residential location and commute times. Microsimulation approaches capture individual heterogeneity and path-dependence over time, building on the theoretical foundations of random utility models and extending them into a time-evolution simulation context. However, disaggregate dynamic models are often complex, computationally demanding -posing challenges for calibration, model updates, and scenario analysis- and data intensive. Large-scale implementations can be slow to run or complex to calibrate, especially when incorporating daily activity-travel simulations. This can hinder policy exploration, as testing many scenarios or running long-term (multi-decade) forecasts becomes time-consuming. Simmonds (2016) emphasise the flexibility of micro models for research but recommended simpler macroscopic models for practitioners to reduce run times. Another challenge is transparency as highly complex agent-based systems can appear opaque to decision-makers, making it hard to trace policy effects, whereas simpler models may more clearly convey causal mechanisms.

Cellular Automata (CA) models represent another dynamic approach, operating at spatially fine-grained geography scale and capable of simulating map-based urban growth patterns while incorporating high-resolution GIS data (Gerber et al., 2018; Lau and Kam, 2005; Von Neumann, 1968). CA use transition probabilities to update land use over time. These models typically include accessibility as a key factor in their transition rules. However, accessibility is often measured using simple proxies, such as the distance to the nearest road or transit line, which ignores the actual performance of the transport system, such as network travel times, congestion, and capacity constraints. As a result, traditional CA models do not simulate transport flows or travel demand explicitly, instead assuming static infrastructure influence. This limits their ability to capture critical feedback loops, such as how new development may generate congestion that in turn affects the desirability of that area. The absence of an explicit transportation component has constrained the policy relevance of early CA models (Xie and Batty, 2004). Recent research has therefore advanced the integration of transport models with CA by running transport simulations in tandem with the land use model (Pinto et al., 2021; Aljoufie et al., 2013; Zhao and Peng, 2012). By explicitly modelling accessibility as an endogenous variable, affected by infrastructure capacity and travel demand, these models better capture the two-way interaction of land development and transportation. While these models might replicate various features of the dynamic and complex land use system, they typically lack behavioural foundations to explain the processes driving it.

Dynamic aggregate approaches adopt a top-down perspective, focusing on stocks and flows at a macro level and the feedback loops among them (Forrester, 1970). Dynamic models make the representation of movement through time explicit. Rather than assuming that each period reflects an equilibrium state, these models simulate flows or transitions - such as changes in population, employment, or land development - year by year (Batty, 1971). Key streams of work in this category include dynamic spatial equilibrium models (Lennox, 2023), system dynamics models (Pfaffenbichler et al., 2008; Swanson and Gleave, 2008), spatial interaction models (Lopane et al., 2023), and flow-based model such as Delta (Feldman and Simmonds, 2005; Simmonds, 1999). DELTA is a rule-based dynamic model that moves beyond static equilibrium by simulating processes of change through a series of interconnected sub-models updated each year. This approach reflects a dynamic equilibrium perspective; rather than assuming the system instantly reaches equilibrium, it allows changes to unfold incrementally. Aggregate dynamic models provide holistic view of the system, remaining particularly relevant for system-level feedback and strategic appraisal, especially when data or computational constraints limit the feasibility of microsimulation.

There are examples of applying System Dynamics (SD) approach to represent urban systems as dynamic entities. Fabolude et al. (2025) reviews recent SD papers with an applications in urban studies. Zhang and

Li (2022); Yu et al. (2018) develop multi-scale models to simulate urban expansion scenarios by embedding multi-scale spatial interactions into the transition rule system of CA, although transport is not incorporated in their modelling framework. Chen et al. (2021); Khosravi et al. (2020); Fontoura et al. (2019) use SD to analyse the influence of policy scenarios on urban transport, focusing on system vulnerability as well as environmental, economic, and traffic variables, while not considering the land use component. urban mobility, thought not considering the land use component.

The MARS model is an example of a LUTI model that employs the SD approach (Pfaffenbichler, 2003). The MARS model has been later coupled with a vehicle fleet model to study the co-evolution of land use transport policies and technological change (e.g., adoption of electric cars) (Ummah, 2019). The work of Haghani et al. (2003b,a) represents an early attempt to apply the SD approach to simultaneous treatment of complex land use and transportation interactions, using a case study of Montgomery County, USA, to evaluate the effects of highway capacity expansion and the resulting changes in land use, which subsequently influence demand and the performance of the transport network. Subsequent studies suggest expansion to multi-modal transport, exploring more sophisticated equations and estimation techniques, and addressing data-related challenges. (Shen et al., 2009) build a high-level SD model to compare high- and low-density land use policies for Hong Kong, concluding that only long-term planning and integrated transit investment could achieve sustainable outcomes. These studies highlight that often, short-term fixes (e.g., building more roads) lead to longer-term unintended consequences (e.g., induced traffic and sprawl), which SD models effectively capture through feedback delays.

SD models build on the tradition of urban dynamics (Forrester, 1970) and systems thinking (Sterman, 2000), emphasising feedback structure -reinforcing or balancing loops- in complex urban systems. There has been still limited application of SD applied in transportation (Pfaffenbichler et al., 2024; Shepherd, 2014). By operating at the zonal level and avoiding individual-level simulation, they run extremely fast, enabling rapid scenario testing and sensitivity analysis that would be prohibitively slow with agent-based models. Their computational efficiency also makes them highly scalable, allowing simulation at national or multi-regional levels without the state-space explosion typical of microsimulation. A further advantage is transparency; SD models explicitly represent feedback loops, often through causal loop diagrams, helping planners and stakeholders qualitatively grasp system dynamics before engaging with quantitative results. Although the limitations of SD models stem from their aggregate nature, the choice of approach depends on the study goals. For example strategic planning and rapid scenario testing often favor SD, while detailed operational forecasting might favor Activity-based models (ABMs) or hybrid approaches. In summary, ABMs and SD offer a trade-off: ABMs provides granularity and behavioural richness at high computational cost, whereas SD offers speed and clarity at the expense of detail.

While the aforementioned studies offer valuable insights into transport and land use interactions, there remains a gap for an agile cross-national decision-support tool that is understandable to policymakers, operates at short daily timesteps to account for processes with varying reaction speeds — from daily travel behaviour changes to long-term infrastructure expansion — and remains computationally efficient. Another challenge lies in the calibration of these models, particularly aggregate ones, which often lack detailed behavioural representation. The application of rigorous estimation methods can enhance the behavioural dimension of the model and improve calibration efficiency.

3 Contributions

Our framework contributes to the state of practice in LUTI modelling by: (i) incorporating cross-national spatial granularity at the zonal level, (ii) dynamic modelling to capture system evolution over time for strategic decision-making, (iii) effectively accounting for time lags between different processes by modelling system states at daily times steps, (iv) eliciting the underlying structure driving system behaviour, and (v) remaining computationally quick. This deliberately designed strategic aggregate model connects long- and short-term urban choices. The developed framework serves as a decision-support tool to understand system behaviour, anticipate future developments, and evaluate the impacts of policy interventions —accounting for the interrelated dynamics of transport, congestion, accessibility, housing markets, land constraints, and population change.

In our study, we estimate certain sub-models using maximum likelihood estimation with the available data, while employing heuristics to calibrate the remaining parameters. A key challenge in SD models is calibration, which is often carried out through trial-and-error procedures, literature-derived elasticities, or expert judgment. Incorporating estimation techniques can enhance behavioural realism and increase the efficiency of parameter calibration. In short, the current study retains the computational efficiency and transparency of the SD approach while extending its scope to a multi-regional scale and grounding its assumptions in localised data. This enables the development of an aggregate model that supports rapid policy evaluation across a wide range of scenarios, remains interpretable to policy makers, and offers scalability for future extensions.

4 Methodology

We develop a system-level framework to jointly model the transport and land use dynamics over a time horizon of multiple years. These modules interact in a time-lagged and bidirectional manner, reflecting the dynamic nature of urban systems. The transport module feeds into the land use module through accessibility, which represents the potential for residents to reach workplaces, services, and other essential opportunities. Accessibility is a key determinant of where people choose to live and work, influencing patterns of urban growth and development. In turn, the land use module is linked back to the transport module through spatial distribution and location choice. These choices, influenced by factors such as housing availability, rent prices, and infrastructure, shape the demand for transport services and the configuration of transportation networks. This bidirectional and time-lagged interaction between transport and land use modules captures how changes in one system (e.g., new transport infrastructure) impact the other, creating a dynamic and interdependent model of urban development. Figure 2 presents the general structure of inter-relationships between these modules.

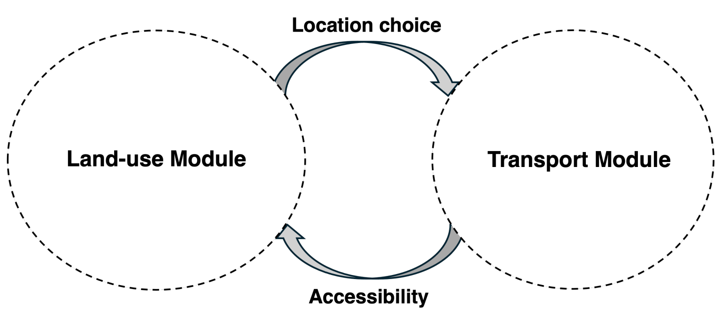

Figure 2: General structure of the integrated framework

This framework builds on the principles of system thinking and system dynamics (Sterman, 2000; Forrester, 1961) and utilises transport manuals, econometric, and behavioural models for quantification. System dynamics is an established discipline developed at MIT, that focuses on understanding and modelling complex, feedback-driven systems over time. The system dynamics approach connects structure and behaviour by explicitly modelling causalities, feedback relationships, and time lags between processes, using dynamic modelling to determine the state of the systems and capture the underlying feedback loop structure of causes and effects. The primary goal of system dynamics models is to understand the underlying structure driving the dynamic behaviour of the system, and to evaluate different policies, which are long-term, macro-level decision rules.

Some specifications of our framework are as follows: (i) The temporal timesteps are set to days. This choice is motivated by the need to capture delays across different urban processes, including short delays such as transport mode choice decisions that may occur within a few days. (ii) The spatial boundaries of the model extend across national borders and are analysed at the level of discrete zones corresponding to existing functional regional divisions such as cantons, cities, or municipalities. (iii) The attractiveness of the region under study and migration patterns are assumed to be exogenously determined. The dynamics of economic prosperity of the region is considered outside the scope of the model. (iv) Travel times and costs for private modes are updated endogenously within the model, whereas those for public transport are treated as exogenous. Public transport fares are typically fixed by regulation, and travel times are assumed externally given. This assumption is justified as part of public transport is rail-based, where travel times remain fixed regardless of demand, while the bus-based component may operate in either mixed traffic or on separated lanes. Since detailed data on this classification are not available and the combined effect on travel times is non-trivial and out of scope of this study, public transport travel times are treated as exogenous. (v) Renting is considered the sole means of satisfying housing demand. (vi) Rent prices are determined endogenously based on the balance of demand and supply at each timestep. (vii) The distribution of workplaces across zones is exogenously given. (viii) The dynamics of land prices fall outside the scope of this study. (ix) The state of the urban system is directly derived through dynamic modelling.

In the remainder of this section, we first present a high-level causal loop diagram to qualitatively illustrate the key feedbacks between transport and residential location choice (Section 4.1). Next, we define the model boundaries and introduce the key model variables in Section 4.2. The quantification of the transport module and the land use module is then detailed in Sections 4.3 and 4.4, respectively.

4.1 Causal loop diagrams

The urban system is composed of various sub-systems including the population, housing, and transport. Our mental models often fail to include the critical feedbacks driving the dynamics of the system. To represent a visual narrative of feedback mechanisms within the system of interest, causal loop diagram consisting of variables connected by arrows denoting the causal influences among the variables are developed using the Vensim PLE software (Ventana Systems, 2025), with the output shown in Figures 3 and 4. In a causal loop diagram, the variable from which the arrow originates represents the cause, while the variable at the arrow's destination is the affected variable. The effect is either positive, where an increase in one variable leads to an increase in the affected variable, indicated by a "+" on the arrow, or negative, where increasing one variable leads to a decrease in another, indicated by a "-" on the arrow. A reinforcing loop (R) amplifies change in the system; a change in one variable leads to further change in the same direction, causing differences to become magnified over time. A balancing loop (B), by contrast, counteracts change; when a variable shifts, corrective actions push it back toward equilibrium, stabilising the system. In causal loop diagrams, delays are indicated by short double slashes "`//`" on the causal arrows.

Consider a region with two residential zones `i` and `j`. In the transport module (Figure 3), an increase in the commute time for residents of zone `i` reduces their accessibility to workplace, which subsequently lowers the relative attractiveness of zone `i`. As the relative appeal of zone `i` declines, the relative attractiveness of residential zone j increases (loop R1). This shift in attractiveness motivates a rise in the relocation of residents from zone `i` to zone j. However, the relocation of population responds gradually to changes, as such moves involve substantial transaction costs, and typically take several months to complete due to factors such as house hunting, negotiations, and settling into new homes. Additionally, there is an information delay; it takes time for residents to perceive the reduced accessibility, and their decision to relocate is influenced by the gradual realisation of these changes in accessibility. As more population move to zone j, the number of daily commutes from zone j also increases, leading to heightened traffic congestion, longer travel times, and overcrowding of public transport system for residents of zone j. This increase in travel times reduces the accessibility of zone j and decreases its relative attractiveness as a place to live (loop B1), controlling the relocation inflow to zone j.

The reduced accessibility can be further moderated by two mechanisms. The first balancing mechanism involves changes in transport mode choices, where residents, facing increased travel time or overcrowding, may switch to alternative transport modes that offer faster or more efficient travel options (loop B2 and B4). The second balancing mechanism considers the expansion of transport infrastructure, which aims to reduce congestion by increasing the capacity of roads, public transport, or other relevant infrastructure (loop B3 and B5). However, the effects of these balancing loops are subject to different time lags. The perception of increased travel time by residents is delayed, as it may take months for them to perceive the change in congestion levels. Even after perceiving the change, it can take several more days for residents to adjust their mode choice accordingly. Additionally, infrastructure expansion involves a significant delay; planning and obtaining the necessary licenses for new infrastructure can take several months to a couple of years, and the construction itself often spans multiple years. The time lags between the initiation of these interventions and their observable impacts on the system vary, adding an additional layer of complexity to the dynamics of the region's transport system.

In the residential relocation module (Figure 4), an increase in the population of zone i raises the demand for housing. In addition to relocation from other zones, population growth in a zone is driven by net immigration to the region and the net birth rate. The latter contributes to a reinforcing loop, as a higher birth rate increases the population, which in turn fuels further population growth (loops R3 and R4). This change in population and thus housing demand is reflected in the dwelling market, specifically in the rental prices and ultimately in the dwelling stock. In particular, dwelling price effects are driven by the interaction between housing demand and supply. When a zone experiences a surge in housing demand while supply remains constant, the average housing surface per person decreases, tightening the market and driving rental prices upward. The effect of population growth on rental prices is not immediate. There is a time lag in how quickly the market adjusts. It may take several months for the rent prices to reflect the increased demand, as the market gradually responds to changing conditions. Once rent prices increase, it may take additional months for residents to perceive the higher costs. This reduces the attractiveness of the zone, prompting some to relocate, which in turn decreases both the population of zone i and its housing demand, ultimately stabilising rent prices (loop B15).

This increase in rental prices, in turn, boosts the attractiveness of housing development in the area. If there is room for new development, an increase in housing demand can lead to an expansion of the housing stock. Rising rents incentivise developers to invest in new residential projects, which over time increases housing supply and moderates rental prices (loop B11). In addition to price incentives, greater market tightness and demand also stimulate further construction (loop B14). However, the housing development process is controlled by land availability (loop B12), and rising land prices (loop B13), both of which play critical roles in initiating housing construction. The expansion of housing supply helps to alleviate the excess demand for housing, but this process is subject to significant time delays, known as construction time lags. These delays mean that the impact of new housing on the market is not immediate. As new homes become available, the excess housing demand in zone i is gradually reduced, leading to stabilisation of residential rent prices (loop B11 and B14). Lower rent prices then increase the relative attractiveness of residential zone i, making it more appealing to potential residents. This, in turn, drives the relocation of individuals to zone i, further influencing the dynamics of competing residential zones.

The dynamics of residential relocation are interdependent, as changes in the attractiveness of one zone, such as zone i, influence the relative appeal of other zones (loop R6). For instance, as more residents move to zone i due to its improved housing availability, the demand for housing in neighbouring zones may decrease, affecting the dynamics in those areas. Consequently, the housing development process in zone i not only impacts its own residential market but also alters the population distribution and competitive balance across other zones.

A number of factors contribute to the complexity of these interactions: on one hand, land development regulations and the decision-making processes of land developers, which shape housing supply and, in turn, influence housing prices; on the other hand, the location choice behaviour of individuals and firms, which determines the spatial distribution of socio-economic activities within the study area. The population movement and relative attractiveness of the residential zones are the common variables between the transport and residential location module, joining these two modules and affecting their inter-related dynamics.

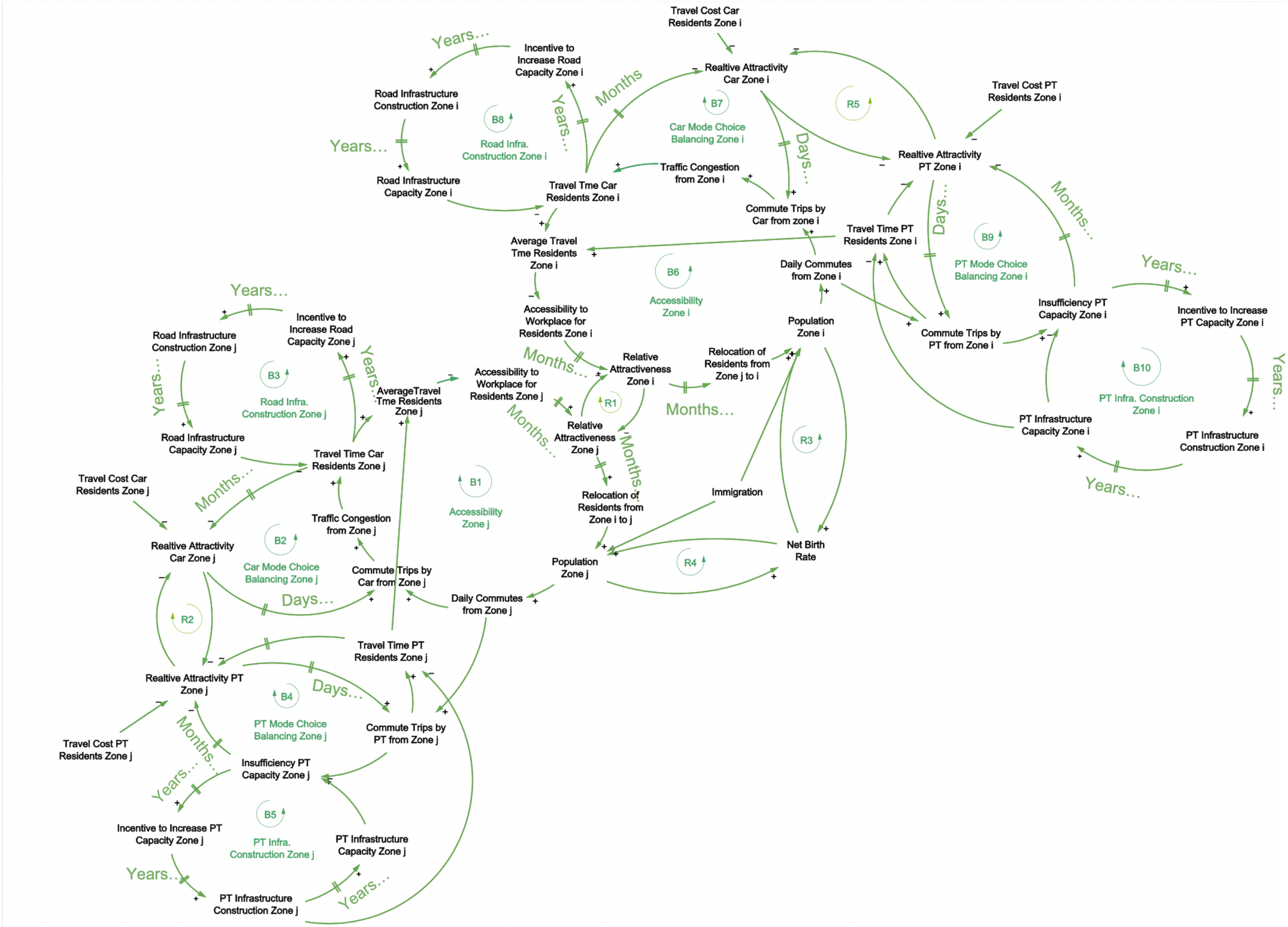

Figure 3: Causal loops in transport

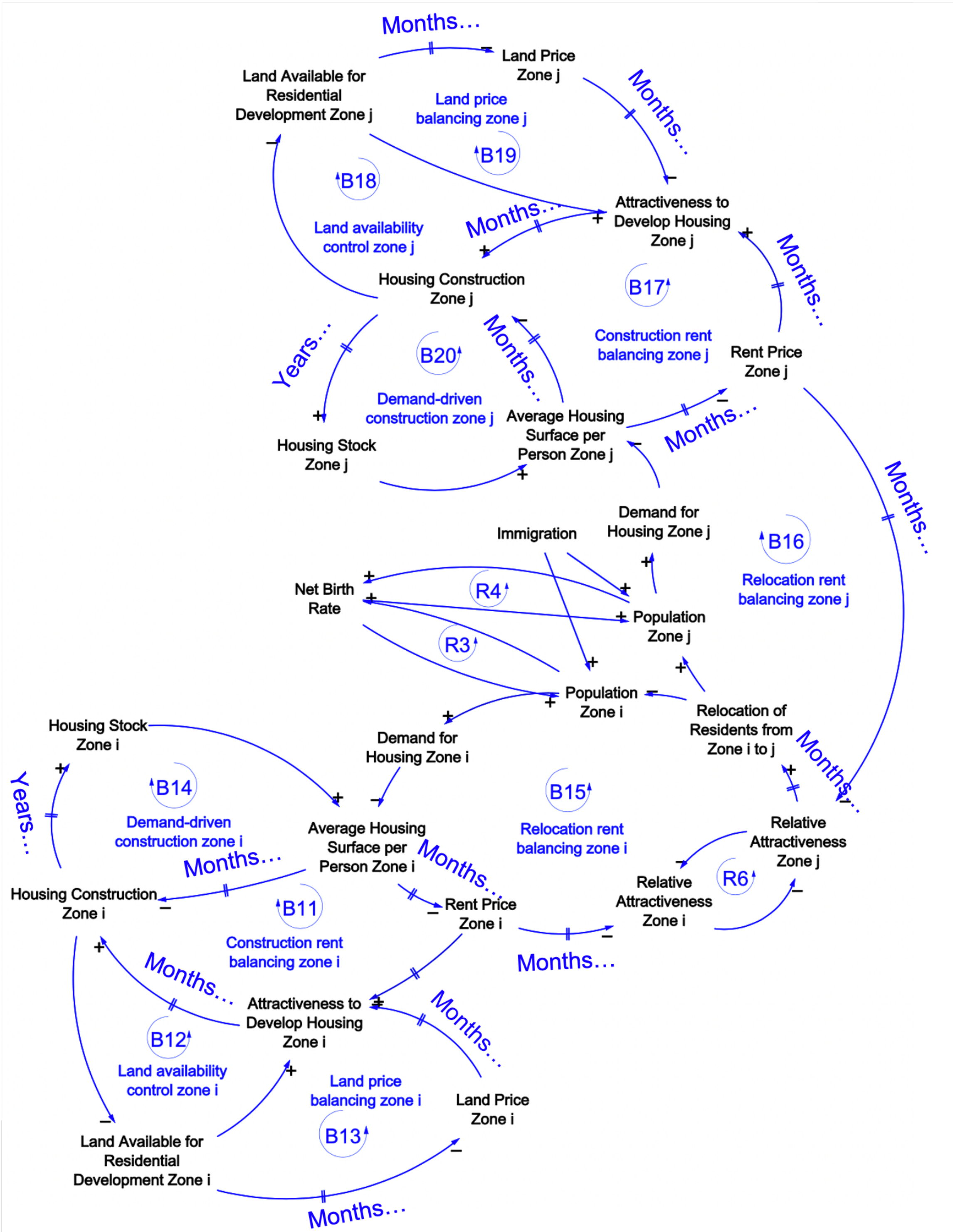

Figure 4: Causal loops in residential relocation

4.2 Model boundary

To clarify the scope of the system dynamics framework, we define the model boundary. Considering this boundary, the variables are classified into three main categories -endogenous, exogenous, and excluded variables- as summarised in Table 1. Endogenous variables can influence the behaviour of the system and are influenced by it. Exogenous variables can influence the behaviour of the system but are not be influenced by it. Excluded variables are omitted from the model either because their influence is assumed negligible or because they lie outside the scope of this study. For clarity, only key variables are listed in the table. It is important to note that the excluded variables presented in the table are merely examples. Many other factors are also not represented in the model, such as taxes and transfers, firms' land demand, goods consumption, and proximity to sellers.

Table 1: Model boundary: Key model variables by types.

Variable Type	**Variable Name**	**Notation**	**Description**	**Unit**
Endogenous	Residents zone i	$N_i^R(t)$	Number of residents in zone i.	Person
	Employed population zone i	$N_i^{Empl}(t)$	Number of employed residents in zone i.	Person
	Residents move-in rate zone i	$mv_i^{in}(t)$	Number of residents moving into zone i at each timestep.	Person/Year [1]
	Residents move-out rate zone i	$mv_i^{out}(t)$	Number of potential residents leaving zone i at each timestep.	Person/Year [1]
	Total potential movers	$N_T^{mv}(t)$	Total number of individuals who may change residence within the study area, composed of net births, migration flows, and out-movers from all zones at each timestep.	Person/Year [1]
	Rent price in zone i	$R_i(t)$	Monthly rent per square meter in zone i.	Euro/m^2/Month
	Residential surface zone i	$S_i(t)$	Total residential floor area in zone i.	m^2
	Housing surface per resident zone i	$S_i^{per}(t)$	Living space available per resident in zone i.	m^2/Person
	Available land to construct zone i	$L_i(t)$	Maximum buildable floor space given current land constraints in zone i.	m^2
	Accessibility zone i	$Acc_i(t)$	A relative measure of a accessibility to workplace for residents of zone i.	-
	Travel time by mode m from zones i to j	$TT_{ij}^m(t)$	Travel time by mode m from zone i to j at morning peak hour.	Min
	Travel cost by car from zones i to j	$TC_{ij}^{PC}(t)$	Total travel cost by car from zone i to j at morning peak hour.	Euro

Continued on next page

(Continued from previous page)

Type	Name	Notation	Description	Unit
Endogenous	Fuel cost for commute by car from zone i to j	$c_{ij}^{fuel}(t)$	Cost of fuel for travel by car from zone i to j.	Euro
	Operating cost for commute by car from zone i to j	$c_{ij}^{maint}(t)$	Vehicle's maintenance and operating cost for travel by car from zone i to j.	Euro
	Toll cost for commute by car from zone i to j	$c_{ij}^{toll}(t)$	Cost of toll fees for travel by car from zone i to j.	Euro
	Number of commuters from zone i	$T_i(t)$	Total number of individuals commuting from zone i during morning peak hour on a workday.	Person/hr
	Number of car commutes from zone i to j	$C_{ij}^{PC}(t)$	Number of cars commuting from zone i to j at morning peak hour on a workday.	Veh/hr
	Number of bus commutes from zone i to j	$C_{ij}^{bus}(t)$	Number of bus-based public transport commutes from zone i to j at morning peak hour on a workday.	Veh/hr
	Number of commuters from zone i to j	$T_{ij}(t)$	Number of commuters from zone i to j at morning peak hour on a workday.	Person/hr
	Number of commuters from zone i to j by mode m	$T_{ij}^{m}(t)$	Number of commuters from zone i to j by mode m at morning peak hour on a workday.	Person/hr
	Road infrastructure capacity from zone i to j	$Cap_{ij}^{PC}(t)$	Relative road corridor capacity between zones i and j, scaled to 1 at baseline ($t = 0$), representing available infrastructure capacity.	-
	PT capacity between zone i and j	$Cap_{ij}^{PT}(t)$	Maximum hourly capacity of public transport services between i and j without overcrowding.	Person/hr
	Car speed between zone i and j	$v_{ij}^{PC}(t)$	Trip-specific speed for travel from zone i to j by car at morning peak hour.	km/hr
Exogenous	Initial Conditions	-	Condition or value of component classes (e.g., residents, housing surface, transport infrastructure) at the beginning of the dynamic model ($t = 0$).	-
	Residents in the study area	$N_T^R(t)$	Total number of residents in the study area of interest.	Person
	Net birth rate	$NB(t)$	Annual net population change from births and deaths in the study area.	Person/Year [1]

Continued on next page

(Continued from previous page)

Type	Name	Notation	Description	Unit
Exogenous	Migration rate	$\mathrm{Mig}_T(t)$	Annual number of individuals migrating to the study area.	Person/Year [1]
	Employment rate zone i	$\lambda_i^{\mathrm{Empl}}(t)$	The proportion of employed residents relative to the working age residents in zone i based on census data.	-
	Share of working-age residents in zone i	$\lambda_i^{\mathrm{WorkAge}}(t)$	The proportion of working-age residents relative to the resident population in zone i based on census data.	-
	Morning peak hour commute rate	$\lambda_{\mathrm{trip}}^{\mathrm{peak}}$	Proportion of total daily commute trips that occur during the morning peak period.	1/hr
	Travel cost by public transport from zone i to j	$\mathrm{TC}_{ij}^{\mathrm{PT}}(t)$	Total travel cost by public transport from zone i to j at morning peak hour.	Euro
	Distance zone i to j	d_{ij}	Total travel distance by car from i to j.	km
	Fuel price	$p^{\mathrm{fuel}}(t)$	Price of fuel per liter in the study area.	Euro/liter
	Fuel consumption	$\eta_f(t)$	Fuel consumption of vehicle per 100 kilometers travelled.	liter/100km
	Maintenance cost per kilometer	$\kappa^{\mathrm{maint}}(t)$	Monetary cost per kilometer to run a vehicle covering expenses such as maintenance, insurance, and depreciation.	Euro/km
	Toll fees	$p^{\mathrm{toll}}(t)$	Monetary charges for using specific roads infrastructures.	Euro
	Car occupancy	$\mathrm{Occ}^{\mathrm{PC}}(t)$	Average number of individuals travelling in a car per trip.	Person/Veh
	Bus occupancy	$\mathrm{Occ}^{\mathrm{bus}}(t)$	Average number of individuals per bus.	Person/Veh
	Attraction of zone j for commuters	$A_j(t)$	Relative attractiveness of zone j as a workplace destination, proxied by the number of jobs in the zone.	-
	Proportion of bus-based commutes	ϕ	Proportion of public transport commutes that use bus.	-
	Free-flow speed	v_{ij}^{FFS}	Free-flow speed of car for travel from zone i to j in uncongested conditions with no traffic interference.	km/hr

Continued on next page

(Continued from previous page)

Type	Name	Notation	Description	Unit
Exogenous	Threshold car speed between zone i and j	$v_{ij}^{\theta,PC}$	Minimum acceptable car speed from zone i to j at morning peak hour; speeds below this threshold trigger infrastructure expansion.	km/hr
	Threshold variables	θ^{PC}, θ^{PT}	Threshold variables denote policy or operational trigger points beyond which infrastructure investment is initiated.	-
	Normative housing surface per person zone i	$A_i^{\text{per,norm}}$	Normative or target residential surface area per person based on planning guidelines or historical standards.	m^2/Person
	Average time living in zone i	τ_i^{mv}	Average time living in zone i before moving to another zone.	Year
	Average building lifetime	τ_{Res}^{life}	Average lifetime of a residential building.	Year
	Residential construction duration	τ_{Res}^{Cnst}	Time lag between the start of construction and the availability of housing.	Year
	Road infrastructure construction duration	τ_{PC}^{Cnst}	Time lag between project initiation and the availability of new road infrastructure.	Year
	Public transport infrastructure construction duration	τ_{PT}^{Cnst}	Time lag between project initiation and the availability of new public transport infrastructure.	Year
	Physical and information time delays	-	Time delays for information perception and physical construction.	-
	Model parameters	-	Parameters used for model calibration and in utility formulations.	-
Excluded	Relative attractiveness of the greater region	-	The relative attractiveness of the study area that affects its annual net external migration rate.	-
	Workplace location	-	The workplace relocation and workplace infrastructure developments dynamics within zones of the study area.	-

[1] Although the model operates with a daily timestep, demographic rates are defined in persons per year for interpretability. Internally, they are converted to daily rates.

4.3 Transport module

The transport module builds on the causal loops presented in Figure 3, situating its formulation within that broader feedback structure. It captures the effects of population growth and the resulting decline in accessibility due to longer travel times (loops B1 and B6 in Figure 3), the long-term balancing role of infrastructure expansion in meeting increased commuting demand (loops B3, B5, B8, and B10 in Figure 3), and the mode choice behaviour of the population that helps to alleviate congestion and capacity insufficiency (loops B2, B4, B7, and B9 in Figure 3). Through these mechanisms, changes in transport demand and supply are linked to changes in accessibility, which in turn influence land use patterns, particularly the spatial distribution of population and economic activities.

The transport module models the travel behaviour of the population and has two models; (i) a travel demand model, and (ii) a travel infrastructure model (supply). The travel demand model captures passenger travels, comprising 4 sub-models (i) trip generation, (ii) trip distribution, (iii) mode choice, and (iv) trip assignment. The travel infrastructure model represents the state and capacity of the transport supply system, including both public transport and road infrastructure. It provides information on available infrastructure and is updated to reflect capacity changes driven by demand. The interaction between the demand and infrastructure models enables the system to account for network conditions, congestion, and accessibility. Figure 5 presents a general scheme of the sub-models and outputs of transport module.

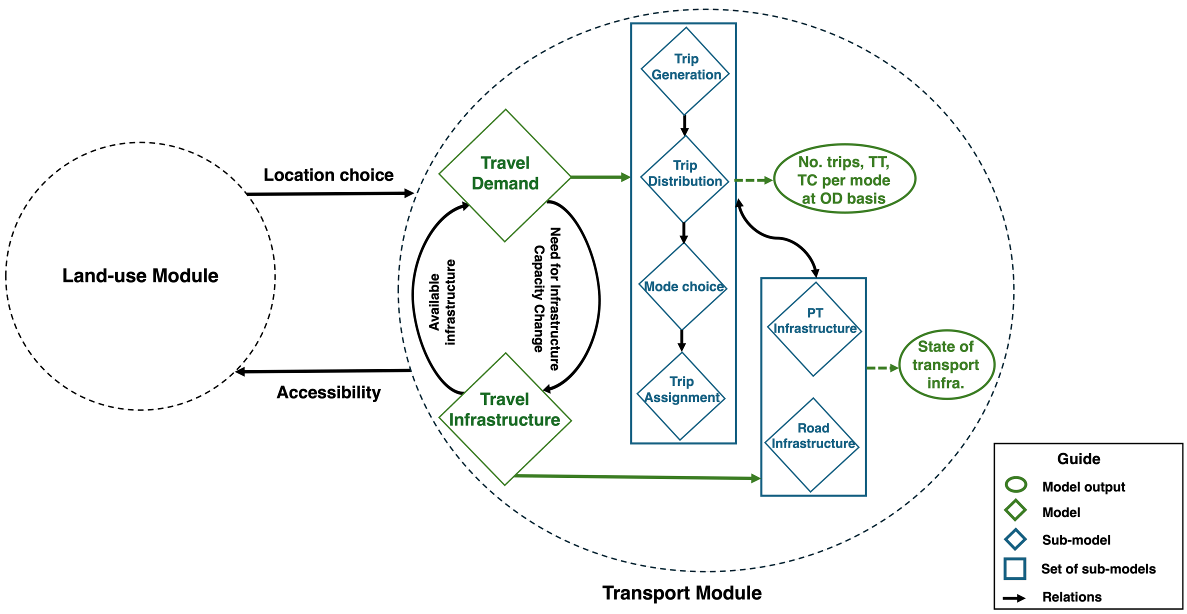

Figure 5: Transport module

4.3.1 Travel demand model

In this framework, travel demand is represented by trip generation volume, expressed as the average number of daily commuters during the morning peak hour. Morning peak is chosen because traffic-related problems are most pronounced at peak times, especially in the morning, which accounts for 45% of daily work trips (Department for transport, directorate for mobility planning, 2018). The trip generation step estimates the number of commuters originating from each zone. Commuting trips are driven by the employed population, with only morning peak-period trips being considered. A trip rate method is applied, in which the number of employed residents in each zone is multiplied by a fixed commute trip rate at morning peak per person on a typical workday. These trip rates are assumed to remain constant per capita and per workday across zones.

$$T_i(t) = N_i^{\text{Empl}}(t)\, \lambda_{\text{trip}}^{\text{peak}} \tag{1}$$

where $T_i(t)$ is the number of morning peak-period commuters originating from zone i at timestep t. $\lambda_{\text{trip}}^{\text{peak}}$ is the average commute trip rate per employed individual during the morning peak hour. $N_i^{\text{Empl}}(t)$ is the number of employed residents in zone i at time t. It is calculated as the product of the resident population in zone i, the employment rate in zone i, and the share of the working-age population in zone i:

$$N_i^{\text{Empl}}(t) = N_i^{R}(t)\, \lambda_i^{\text{WorkAge}}(t)\, \lambda_i^{\text{Empl}}(t) \tag{2}$$

where $N_i^{R}(t)$ is the number of residents in zone i at time t, $\lambda_i^{\text{WorkAge}}(t)$ is the ratio of working-age population (15-64 years) in zone i, and $\lambda_i^{\text{Empl}}(t)$ is the employment rate among working age population in zone i, obtained from census data.

In trip distribution, the trips generated in the trip generation step are allocated to destination zones, determining the spatial pattern of commuting flows. The trip distribution sub-model calculates the proportion of commute trips to each chosen destination from a given origin. This step is central to four-step travel demand models, as it links trip origins with plausible destinations based on opportunities and travel impedance. This allocation is performed using a gravity model (Ortuzar and Willumsen, 2011), a widely used spatial interaction model in transportation planning to estimate how trips are distributed from origins to destinations. It assumes that the number of trips between two zones is directly proportional to the attractiveness of the destination and inversely proportional to the generalised travel cost between them. Given the total number of trip productions $T_i(t)$ from each origin zone i, the raw attractiveness values $A_j(t)$ for each destination zone j (e.g., number of jobs in zone j), and the generalised travel cost $\text{GC}_{ij}(t)$, the production-constrained (singly constrained) gravity model is expressed as folows:

$$T_{ij}(t) = T_i(t) \frac{A_j(t)\, \text{FF}(\overline{\text{GC}}_{ij}(t))}{\sum_k A_k(t)\, \text{FF}(\overline{\text{GC}}_{ik}(t))} \tag{3}$$

where $T_i(t)$ is the number of commuters from zone i at morning peak. $T_{ij}(t)$ denotes the number of morning peak hour commuters from origin zone i to destination zone j. The function $\text{FF}(\overline{\text{GC}}_{ij}(t))$ represents a deterrence function, which is a monotonically decreasing function of perceived generalised cost. It captures the diminishing likelihood of choosing more distant or expensive destinations. The denominator $\sum_k A_k(t)\, \text{FF}(\overline{\text{GC}}_{ik}(t))$ serves as a normalisation term, ensuring that the total number of trips from each origin zone i are proportionally distributed across all destinations based on their relative weighted attractiveness. Since this model is singly constrained, only origin totals are preserved. Destination totals emerge endogenously as destinations compete for trips based on their attractiveness adjusted by travel impedance.

The form of $\text{FF}(\overline{\text{GC}}_{ij}(t))$ is typically chosen based on the trip purpose and empirical evidence of travel behaviour. For commute trips, an exponential decay form is commonly applied as Equation 4.

$$\text{FF}(\overline{\text{GC}}_{ij}(t)) = e^{\beta_{\text{GC}} \overline{\text{GC}}_{ij}(t)} = e^{\beta_{\text{GC}} \left(\beta_{\text{TT}}^{\text{GC}} \overline{\text{TT}}_{ij}^{(\Delta t_{\text{perc,transp}})}(t) + \beta_{\text{TC}}^{\text{GC}} \overline{\text{TC}}_{ij}^{(\Delta t_{\text{perc,transp}})}(t) \right)} \tag{4}$$

where β_{GC} is the impedance parameter that reflects the sensitivity of trip distribution to generalised cost, estimated to fit data using Hyman method (Hyman, 1969). The generalised cost, $\overline{\text{GC}}_{ij}(t)$, is expressed as a money-metric utility, composed of perceived travel time $\overline{\text{TT}}_{ij}^{(\Delta t_{\text{perc,transp}})}(t)$, and perceived travel cost $\overline{\text{TC}}_{ij}^{(\Delta t_{\text{perc,transp}})}(t)$. These quantities are averaged over a perception time window $\Delta t_{\text{perc,transp}}$, capturing the information delay in the decision-making process, reflecting how travel time and cost are perceived by commuters over a specific time period rather than instantaneously. The parameter $\beta_{\text{TT}}^{\text{GC}}$ is the parameter the travel time, denoting the willingness to pay, and allows for the conversion of travel time into monetary units. $\beta_{\text{TC}}^{\text{GC}}$ is parameter of travel cost, normalised to -1 to maintain consistency with the money-metric utility formulation.

Once the generated trips are distributed across destination zones, the mode choice step determines how these trips are divided among available transportation modes. The mode choice sub-model calculates the proportion of total commuters between each origin-destination pair allocated to each mode. The mode choice sub-model uses a logit specification, to relate the attractiveness of each mode to its perceived characteristics. Each transport mode is associated with a utility function that captures the perceived travel cost and travel time for that mode. Importantly, both travel time and cost are perceived through a temporal filter, averaged over a perception window , $\Delta t_{\text{perc,transp}}$, that reflects the delayed adjustment to changes in travel conditions. The resulting number of commuters by mode is given by:

$$T_{ij}^{m}(t) = T_{ij}(t)\frac{e^{\mu V_{ij}^{m}(t)}}{\sum_{m'} e^{\mu V_{ij}^{m'}(t)}} \tag{5}$$

where $T_{ij}^{m}(t)$ denotes the number of morning peak-period commuters from zone i to j using mode m. μ is a scale parameter. $V_{ij}^{m}(t)$ is the systematic utility associated with mode m for the same origin-destination pair, $(i$,$j)$. The utility function $V_{ij}^{m}(t)$ is defined as:

$$V_{ij}^{m}(t) = \text{ASC}^{m} + \beta_{\text{TT}}^{m}\overline{\text{TT}}_{ij}^{(\Delta t_{\text{perc,transp}}),m}(t) + \beta_{\text{TC}}^{m}\overline{\text{TC}}_{ij}^{(\Delta t_{\text{perc,transp}}),m}(t) \tag{6}$$

where $\overline{\text{TT}}_{ij}^{(\Delta t_{\text{perc,transp}}),m}(t)$ is the perceived travel time from origin i to destination j by mode m, averaged over the perception time window $\Delta t_{\text{perc,transp}}$. $\overline{\text{TC}}_{ij}^{(\Delta t_{\text{perc,transp}}),m}(t)$ is the perceived travel cost between zones i and j by mode m, smoothed over the same perception time window, $\Delta t_{\text{perc,transp}}$. β_{TT}^{m} and β_{TC}^{m} are mode-specific utility parameters reflecting the disutility of travel time and travel cost, respectively. ASC^{m} is the alternative specific constant, representing the baseline preference for choosing mode m beyond accounted travel attributes.

The travel time by car between each origin destination pair at morning peak-hour can be estimated using the fundamental relationship between speed and distance, as Equation 7.

$$\text{TT}_{ij}^{\text{PC}}(t) = \frac{d_{ij}}{v_{ij}^{\text{PC}}(t)} \cdot 60 \tag{7}$$

where $\text{TT}_{ij}^{\text{PC}}(t)$ is the travel time by car from i to j. d_{ij} is the total travel distance by car from zone i to j. $v_{ij}^{\text{PC}}(t)$ denotes the trip-specific speed for travel from zone i to j by car. A BPR-type speed–flow relationship is applied to express speed as a function of demand–capacity ratio, using the standard functional form found in macroscopic travel demand models (e.g., Ortuzar and Willumsen (2011)). The commute speed by car between zones i and j at each timestep t is given by:

$$v_{ij}^{\text{PC}}(t) = \frac{v_{ij}^{\text{FFS}}(t)}{1 + \alpha \cdot (\text{DF}_{ij}^{\text{PC}}(t))^{\beta}} \tag{8}$$

where $v_{ij}^{\text{FFS}}(t)$ denotes the free-flow speed by car for travel from zone i to j, representing the speed of vehicles under low-volume conditions, when drivers are free to travel at their desired speed without being constrained by other vehicles or downstream traffic controls. This speed approximates the theoretical condition where both traffic density and flow rate are near zero. In practice, posted speed limits are often used as a proxy for free-flow speed. $\text{DF}_{ij}^{\text{PC}}(t)$ is demand factor of corridor from i to j during the morning peak period at timestep t. Parameters α and β are empirical coefficients, set to $\alpha = 0.15$ and $\beta = 4$ (California Department of Transportation, 2022). $\text{DF}_{ij}^{\text{PC}}(t)$ is derived based on Equation 9.

$$\text{DF}_{ij}^{\text{PC}}(t) = \text{DF}_{ij}^{\text{PC}}(0)\frac{\text{Cap}_{ij}^{\text{PC}}(0)}{\text{Cap}_{ij}^{\text{PC}}(t)} \cdot \frac{C_{ij}^{\text{PC}}(t) + C_{ij}^{\text{bus}}(t)}{C_{ij}^{\text{PC}}(0) + C_{ij}^{\text{bus}}(0)} \tag{9}$$

where $\text{Cap}_{ij}^{\text{PC}}(t)$ denotes the relative road corridor capacity from zone i to j at timestep t. $\text{Cap}_{ij}^{\text{PC}}(t)$ is a dimensionless, non-negative variable defined on a relative scale with respect to the road infrastructure capacity at timestep 0, $\mathrm{Cap}_{ij}^{PC}(t) \in (0, \infty)$. A value of $\mathrm{Cap}_{ij}^{PC}(t) = 1$ indicates that the road capacity is equal to the baseline capacity at timestep 0. A value of $\mathrm{Cap}_{ij}^{PC}(t) = 0$ represents a fully non-functional (closed) corridor. Values greater than 1 indicate an increased capacity relative to the base case (e.g., due to infrastructure expansion), while values less than 1 represent a reduced capacity (e.g., due to disruptions or degradation). The capacity may vary over time, taking values above or below 1 depending on infrastructure development or deterioration of the network. $C_{ij}^{PC}(t)$ is the number of car-based commutes from i to j at timestep t, calculated using the morning peak origin-destination commuter flows and car occupancy as Equation 10.

$$C_{ij}^{PC}(t) = \frac{T_{ij}^{PC}(t)}{\mathrm{Occ}^{PC}(t)} \tag{10}$$

where $T_{ij}^{PC}(t)$ is the number of morning peak-period commuters from zone i to j using private vehicle, and $\mathrm{Occ}^{PC}(t)$ is the average car occupancy, expressed as the number of people per car.

In Equation 9, $C_{ij}^{bus}(t)$ denotes the number of bus-based public transport commutes from i to j at timestep t. It is computed based on the total number of public transport commuters during the morning peak, $T_{ij}^{PT}(t)$, the proportion of those using buses with mixed traffic ϕ, and the average occupancy of buses $\mathrm{Occ}^{bus}(t)$ expressed as average number of people per bus, as follows:

$$C_{ij}^{bus}(t) = \frac{\phi\ T_{ij}^{PT}(t)}{\mathrm{Occ}^{bus}(t)} \tag{11}$$

$\mathrm{DF}_{ij}^{PC}(0)$ is the initial demand factor, used to initialise the transport model and calculated as:

$$\mathrm{DF}_{ij}^{PC}(0) = \sqrt[\beta]{\frac{v_{ij}^{FFS}(0) - v_{ij}^{PC}(0)}{\alpha \cdot v_{ij}^{PC}(0)}} \tag{12}$$

where $v_{ij}^{PC}(0)$ is the trip-specific speed at morning peak from zone i to j by car at timestep 0. The trip-specific speed can be computed as:

$$v_{ij}^{PC}(0) = \frac{d_{ij}}{\mathrm{TT}_{ij}^{PC}(0)} \cdot 60 \tag{13}$$

where d_{ij} is the commute distance from zone i to j. $\mathrm{TT}_{ij}^{PC}(0)$ is the travel time from i to j by car at timestep 0, which is estimated based on Google maps data.

The travel cost for private car trips, denoted as $\mathrm{TC}_{ij}^{PC}(t)$, comprises multiple components, calculated as Equation 14.

$$\mathrm{TC}_{ij}^{PC}(t) = c_{ij}^{fuel}(t) + c_{ij}^{maint}(t) + c_{ij}^{toll}(t) \tag{14}$$

where $c_{ij}^{fuel}(t)$ represents the fuel cost, $c_{ij}^{maint}(t)$ refers to the vehicle's maintenance and operating costs, $c_{ij}^{toll}(t)$ accounts for toll charges and road pricing. The fuel cost component, $c_{ij}^{fuel}(t)$, can be estimated as Equation 15.

$$c_{ij}^{fuel}(t) = 100\ d_{ij}\ \eta_f(t)\ p^{fuel}(t) \tag{15}$$

where d_{ij} is the travel distance between zones i and j in kilometers, $\eta_f(t)$ is the fuel consumption of vehicle expressed as liter per hundred kilometers (liter/100km). $p^{fuel}(t)$ is the fuel price per unit (Euro/liter).

The vehicle operating cost, $c_{ij}^{maintenance}(t)$, covers wear-and-tear expenditures such as maintenance, tires, insurance, and depreciation, and is estimated as:

$$c_{ij}^{maint}(t) = d_{ij}\ \kappa^{maint}(t) \tag{16}$$

where $\kappa^{\mathrm{maint}}(t)$ denotes monetary cost per kilometer to run a vehicle covering expenses such as maintenance, insurance, and depreciation (Euro/km).

The cost of toll charges for car travel from zone i to j, denoted as $c_{ij}^{\mathrm{toll}}(t)$, is calculated by summing the toll fees p^{toll} associated with all tolled links along the shortest or assigned path between the two zones.

$$c_{ij}^{\mathrm{toll}}(t) = \sum_{i}^{j} p^{\mathrm{toll}}(t) \tag{17}$$

For public transport modes, travel costs are defined exogenously, as they are typically regulated. Travel times are primarily derived exogenously from observed performance data. However, to account for the fact that some bus-based services operate in mixed traffic and are thus affected by road congestion, a weighted average is applied. This average combines the exogenously defined travel time with an endogenously calculated travel time that reflects current road traffic conditions. The weight assigned to each component depends on the proportion of the public transport service that is affected by general traffic conditions. For instance, corridors with services operating entirely on dedicated lanes (e.g., trams or buses with exclusive right-of-way) rely on exogenous travel time data. By contrast, corridors with bus services that share road space with private vehicles are more sensitive to congestion and therefore incorporate endogenous travel time estimates, weighted by the share of public transport operating in mixed traffic within the corridor. The travel cost for public transport is defined exogenously and regulated.

Trips are analysed at the corridor level, with one corridor defined between each origin–destination pair. Consequently, the trip assignment stage is simplified, and only a single route is considered between each pair of zones.

In the travel demand model, at each timestep, the transport flows at an origin-destination basis by each transport mode, the average travel times and travel costs between each origin-destination pair per transport mode are modelled.

4.3.2 Travel infrastructure model

In the transport infrastructure development model, the decision to increase the road transport infrastructure capacity is determined with a set of rules based on the commute speed by car at morning peak and number of commutes as follows:

$$\text{If } \frac{\overline{C}_{ij}^{PC,(\Delta t_{\mathrm{dec,transp}})}(t)}{C_{ij}^{PC}(0)} \geq 1 + \theta^{PC} \text{ and } \overline{\nu}_{ij}^{PC,(\Delta t_{\mathrm{dec,transp}})}(t) \leq \nu_{ij}^{\theta,PC}, \text{ then } \mathrm{Cap}_{ij}^{PC*}(t) = \frac{\overline{C}_{ij}^{PC,(\Delta t_{\mathrm{dec,transp}})}(t)}{C_{ij}^{PC}(0)} \tag{18}$$

where $\overline{C}_{ij}^{PC,(\Delta t_{\mathrm{dec,transp}})}(t)$ is the perceived average number of commutes during the morning peak from zone i to j at timestep t, averaged over the decision time window $\Delta t_{\mathrm{dec,transp}}$. This smoothing accounts for the fluctuations in commute patterns over time and provides a more stable estimate for decision-making regarding road expansion. $C_{ij}^{PC}(0)$ is number of commutes at morning peak from i to j at the start of the modelling ($t = 0$). θ^{PC} is a threshold for road capacity expansion (e.g., 0.25), indicating when the road needs expansion based on changes in the number of morning peak commutes. $\overline{\nu}_{ij}^{PC,(\Delta t_{\mathrm{dec,transp}})}(t)$ is the perceived trip-specific speed by car at the morning peak from zone i to j at timestep t, averaged over the decision time window $\Delta t_{\mathrm{dec,transp}}$. $\nu_{ij}^{\theta,PC}$ is the minimum acceptable threshold car commute speed. If the perceived trip-specific car speed falls below this threshold, it suggests that the road is congested and needs to be expanded. $\mathrm{Cap}_{ij}^{PC*}(t)$ is the desired road capacity from zone i to j at timestep t, based on the decision criteria. Once initiated, transport infrastructure come into operation after a time delay of construction time, $\tau_{PC}^{\mathrm{Cnst}}$.

Public transport infrastructure development follows a similar rule-based approach, driven by demand during the morning peak and the capacity constraints of existing public transport links between zones. Once initiated, transport infrastructure come into operation after a time delay of construction time, τ_{PT}^{Cnst}.

In the travel infrastructure model, the state of the transport infrastructure at each timestep is modelled and updated. Using the outputs from transport module, the accessibility measure is computed, linking the transport module back to the land use module.

The accessibility measure is derived by integrating outputs from the transport and land use modules. Accessibility is measured using a Hansen-type indicator (Miller, 2020), which quantifies the ease of reaching employment opportunities. This measure is based on the gravity model, which assumes that accessibility depends on both the number of available jobs at destination and the impedance of travel (Ibeas et al., 2013; Coppola and Nuzzolo, 2011). The accessibility measure for residents of each zone i, denoted as $Acc_i(t)$, is calculated as shown in Equation 19.

$$Acc_i(t) = \sum_j A_j(t)\, e^{\beta_{TT}^{Acc}\overline{TT}_{ij}(t)} \tag{19}$$

where $A_j(t)$ is the number of jobs in destination zone j, $\overline{TT}_{ij}(t)$ is average travel time at morning peak hour for trip from zone i to j at timestep t, and β_{TT}^{Acc} is a decay parameter reflecting sensitivity of accessibility measure to travel time. The exponential decay function captures how accessibility declines with increasing travel time. Higher values of accessibility indicate greater access to employment opportunities within reasonable travel times. We focus on accessibility to workplaces for two main reasons. First, access to employment is a key factor in residential location choice models from a theoretical perspective (Alonso, 1964; Lowry, 1964). It influences individuals' job prospects, supports activity participation, and affects overall quality of life (Niedzielski and Eric Boschmann, 2014). Second, employment accessibility is strongly correlated with accessibility to shopping and leisure opportunities (Baraklianos et al., 2020).

4.4 Land use module

The land use module models the dynamics of residential and workplace relocation and development, consisting of two models; (i) a residential model, and (ii) a workplace model (Figure 6). The residential and workplace location models determine the placement of population and jobs. These models adjust previous spatial distributions in response to changing conditions. In the current framework, we focus only on the residential model and assume the workplace model as given and exogenous. In further operational extensions of the framework, the workplace model can be endogenised. The residential model has two sub-models; (i) a residential relocation sub-model (demand), and (ii) a housing development sub-model (supply). Residential location choices are influenced by factors such as housing supply, accessibility, rental prices, all of which are endogenously determined within the model. The major factor for housing development is the increase in housing demand due to increase in population. Housing development is also influenced by housing market factors such as housing prices and is constrained by land available for residential development.

The residential model builds on the causal loops presented in Figure 4, situating its formulations within that broader feedback structure. It captures the effects of population growth (loops R3 and R4 in Figure 4), including the resulting surge in housing demand, increased market pressure, and rent dynamics that influence the relative attractiveness of zones for residents (loops B15 and B16 in Figure 4). It also reflects the long-term balancing role of housing developments (loops B11, B14, B17, and B20 in Figure 4), as well as constraints from land availability (loops B12 and B18 in Figure 4). An analysis of land price dynamics lies beyond the scope of this study (loop 13 and B19 in Figure 4). Through these mechanisms, changes in housing demand and supply translate into shifts in the number of residents in each zone and commuting demand, which in turn influence transport patterns.

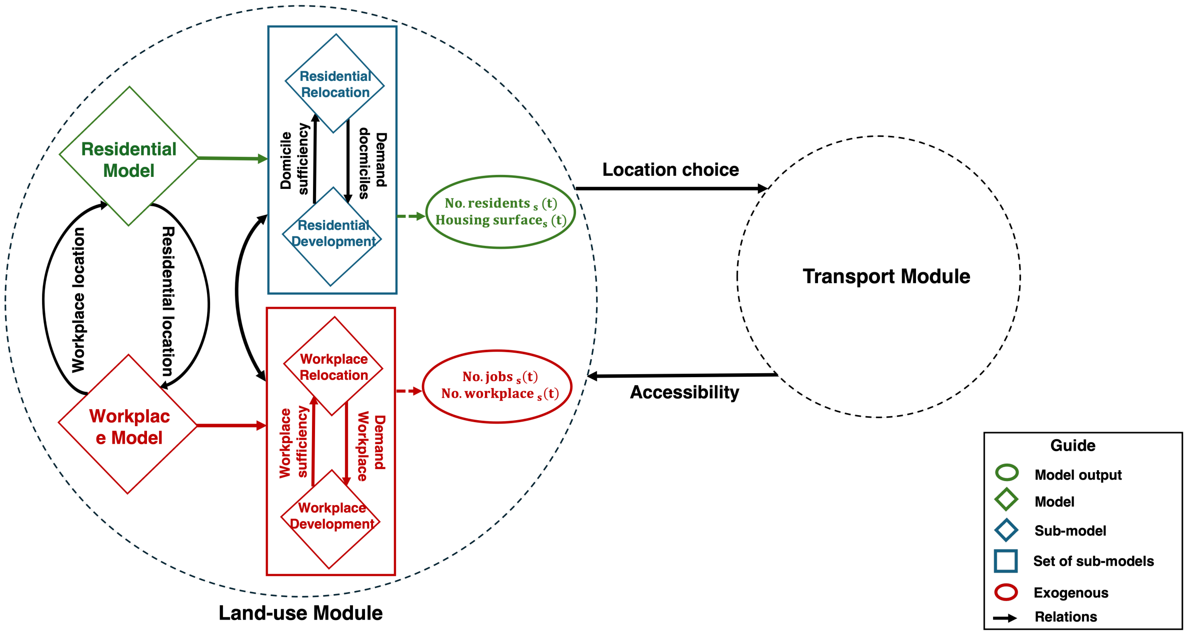

Figure 6: land use module

4.4.1 Residential relocation sub-model

The residential relocation sub-model identify the the number of residents who will relocate within the current timestep and assigns them to zones within the study area. The residential relocation is formulated as a rate-based logit model. Once the potential number of residents to relocate is estimated, the location choice sub-model assigns them to specific destination zones using a multinomial logit specification. The relocation of residents within the study area is modelled through three steps:

(i) Out-migration of residents: The potential number of residents relocating from each zone is estimated based on the average duration of residence.

$$mv_i^{out}(t) = \frac{N_i^R(t)}{\tau_i^{mv}} \tag{20}$$

where $mv_i^{out}(t)$ is the move-out rate from zone i, $N_i^R(t)$ is the number of residents in zone i at timestep t, and τ_i^{mv} represents the average length of residence in zone i, estimated from housing survey data.

(ii) Pooling of movers: At each timestep, the total pool of potential movers in the region consists of net births, net migration into the study area, and out-migration from all zones:

$$N_T^{mv}(t) = NB(t) + Mig_T(t) + \sum_i mv_i^{out}(t) \tag{21}$$

where $N_T^{mv}(t)$ is the total number of potential movers in the greater region. $NB(t)$ is the net birth rate, and $Mig_T(t)$ is the net migration rate to the study area, both derived exogenously from population census data.

(iii) Allocation of movers to zones: Movers are distributed across residential zones using a logit model that accounts for the characteristics of destination zones, such as perceived accessibility to workplace and rent prices. Additional proxy for area quality (e.g., distance to the city center, average income of residents, etc) may also be included.

$$\mathrm{mv}_i^{\mathrm{in}}(t) = N_T^{\mathrm{mv}}(t) \frac{e^{\mu V_i(t)}}{\sum_k e^{\mu V_k(t)}} \tag{22}$$

where μ is a scale parameter, and the systematic utility of each zone, $V_i(t)$, is defined as follows:

$$V_i(t) = \mathrm{ASC}_i + \beta_{\mathrm{Rent}}\, \overline{R}_i(t)^{(\Delta t_{\mathrm{perc,Res}})} + \beta_{\mathrm{Acc}}\, \overline{\mathrm{Acc}}_i^{(\Delta t_{\mathrm{perc,Res}})}(t) \tag{23}$$

ASC_i is the alternative specific constant associated with zone i. $\overline{R}_i(t)^{(\Delta t_{\mathrm{perc,Res}})}$ denotes the perceived monthly rent per square meter in zone i at timestep t, averaged over the perception delay window, $\Delta t_{\mathrm{perc,Res}}$. This temporal averaging captures information delays and smooths short-term fluctuations in rent over the specified period. $\overline{\mathrm{Acc}}_i^{(\Delta t_{\mathrm{perc,Res}})}(t)$ represents the perceived accessibility to workplace from zone i, averaged over the same perception time window, $\Delta t_{\mathrm{perc,Res}}$. This smoothing accounts for temporal changes in accessibility, again reflecting the lag in perception. The parameters β_{Rent} and β_{Acc} calibrated from observed data, capture the sensitivity of residential utility to perceived rent and accessibility, respectively. In the allocation of potential movers, it is assumed that the choice of destination is not influenced by the location of the current domicile of movers.

Rent prices are determined endogenously in the model based on the available surface area per resident in each zone. At each timestep, a desired rent price $R_i^*(t)$ is computed as a function of the tightness of the housing market in zone i, defined as the ratio between the current surface area per person and a normative benchmark for that zone:

$$\begin{aligned} R_i^*(t) &= R_i(t) \cdot f^R\left(\frac{\overline{S}_i^{\mathrm{per},(\Delta t_{\mathrm{dec,Res}})}(t)}{S_i^{\mathrm{per,norm}}}\right) \\ &= R_i(t) \cdot f^R\left(\frac{\overline{S}_i^{(\Delta t_{\mathrm{dec,Res}})}(t)/\overline{N}_i^{R,(\Delta t_{\mathrm{dec,Res}})}(t)}{(S_i/N_i^R)^{\mathrm{norm}}}\right) = R_i(t) \cdot f^R\left(\frac{1}{\overline{\mathrm{Tight}}_i^{(\Delta t_{\mathrm{dec,Res}})}(t)}\right) \end{aligned} \tag{24}$$

where $R_i(t)$ is the monthly rent price per square meter in zone i at timestep t, $S_i(t)$ is the residential surface area, and $N_i^R(t)$ is the number of residents in zone i at timestep t. $\overline{S}_i^{\mathrm{per},(\Delta t_{\mathrm{dec,Res}})}(t)$ denotes the perceived residential surface area per person in zone i at timestep t over the decision time window $\Delta t_{\mathrm{dec,Res}}$. $S_i^{\mathrm{per,,norm}}$ is the normative or target residential surface area per person in zone i, based on planning guidelines or historical standards. $\frac{S_i^{\mathrm{per,norm}}}{S_i^{\mathrm{per}}(t)}$ represents the tightness of the housing market in zone i, quantifying how tight or loose the market is —that is, whether housing is scarce or abundant relative to the number of people needing it. The function f^R expresses how deviations from the target density level influence the desired rent price. A high tightness value indicates overcrowding (low surface area per person), which drives the desired rent price upward; conversely, low tightness suggests abundance of housing and lowers the desired rent. The function f^R is a nonlinear lookup function calibrated to replicate historical rent prices across zones. The actual rent price, $R_i(t)$, does not adjust instantaneously to the desired level. Instead, it evolves gradually over time, reflecting the inertia of real estate markets. The rate of change in the rent price is governed by:

$$\frac{dR_i(t)}{dt} = \frac{R_i^*(t) - R_i(t)}{\tau_{\mathrm{Rent}}^{\mathrm{adj}}} \tag{25}$$

where $\tau_{\mathrm{Rent}}^{\mathrm{adj}}$ is the time lag associated with rent adjustment. This formulation captures the delayed response of rent prices to supply–demand imbalances.

4.4.2 Residential development sub-model

The housing development sub-model determines the expansion of residential floor space in each zone, accounting for both demand-driven triggers and physical constraints. This process is guided by planning policy inputs and is influenced by rent levels, residential densities, and the availability of land designated for residential construction. The decision to develop is based on three key factors: (i) housing demand, (ii) rent prices, and (iii) availability of land for residential construction. Housing surface tightness is defined in terms of the ratio between a desired/normative benchmark and the current surface area per resident. When this ratio goes over one —indicating overcrowding— the pressure to develop increases. Higher rent prices provide financial incentives for development, while land availability constrains the total amount that can be built. Housing development takes one or more years to complete. As a result, newly constructed dwellings become available only after a predefined construction time lag. As new housing is added, the overall floor space increases, raising the surface area per resident. This reduces development pressure and contributes to stabilising or lowering rent levels.

Figure 7 presents a system dynamics stocks and flow for residential development mechanism. New housing developments enter the system through the housing development rate, accumulates in the housing under-construction stock, and is added to the available housing surface after a construction delay. The available housing surface gradually ages and depreciates based on the average building lifetime.

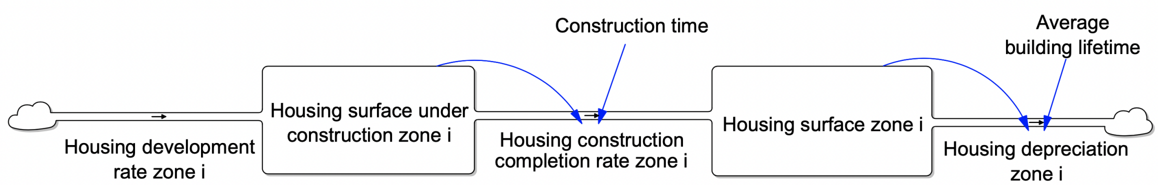

Figure 7: Scheme of housing development dynamics in zone i.

The desired housing surface, $A_i^*(t)$ is computed as a function of the existing housing surface in decision time t, the surface area available per resident relative to a normative benchmark, and rent levels. Specifically, when the housing surface per resident is low or rent prices are high, the desired housing surface increases.

$$S_i^*(t) = S_i(t) \cdot f^S \left(\frac{\overline{S}_i^{\text{per},(\Delta t_{\text{dec,Res}})}(t)}{S_i^{\text{per,norm}}} \right) \cdot \left(\frac{\overline{R}_i^{(\Delta t_{\text{dec,Res}})}(t)}{R_i^{\text{ref}}} \right)^{\Phi} \tag{26}$$

where $S_i(t)$ is the housing surface in zone i at decision time t. $\overline{S}_i^{\text{per},(\Delta t_{\text{dec,Res}})}(t)$ is the perceived housing surface per resident over decision time period $\Delta t_{\text{dec,Res}}$. $S_i^{\text{per,norm}}$ is the normative per capita housing surface. The function f^S is a nonlinear lookup function, capturing how development pressure responds to deviations from the target surface area per person. The function f^S increases as the surface per resident decreases, reflecting growing development pressure when space becomes scarce. $\overline{R}_i^{(\Delta t_{\text{dec,Res}})}(t)$ is the perceived rent price smoothed over the decision time window $\Delta t_{\text{dec,Res}}$. R_i^{Ref} is a reference rent, and Φ denotes the elasticity of housing supply with respect to rent price. This formulation means that incentive for development increases when living space is tight and rent prices are high.

This desired surface is compared to the existing stock to determine the rate at which new housing enters construction. The actual construction inflow is limited by land availability $L_i(t)$, leading to the formulation:

$$\frac{dS_i^{\text{in construction}}(t)}{dt} = \min\left(\max\left(S_i^*(t) - S_i(t), 0\right), L_i(t)\right) \tag{27}$$

where $L_i(t)$ is the maximum buildable floor space given current land constraints. This equation ensures that construction only occurs if the desired surface exceeds the current surface ($S_i^*(t) > S_i(t)$) and that it remains within the land constraint.

Once initiated, housing remains under construction for a duration of construction time, $\tau_{\text{Res}}^{\text{Cnst}}$, as shown in the central stock of the diagram in Figure 7. After this delay, housing is added to the built environment at a completion rate. This corresponds to the rightward flow in the diagram from the "Housing surface under construction" to the "Housing surface" stock.

$$\frac{dS_i(t)}{dt} = \frac{S_i^{\text{in construction}}(t)}{\tau_{\text{Res}}^{\text{Cnst}}} - \frac{S_i(t)}{\tau_{\text{Res}}^{\text{life}}} \tag{28}$$

where $\tau_{\text{Res}}^{\text{Cnst}}$ is the average construction time delay. Finally, assuming a constant-rate decay, housing depreciates over time and exits the stock at a rate proportional to the average building lifetime, $\tau_{\text{Res}}^{\text{life}}$.

Together, these equations describe the dynamics of residential development: from identifying the need for new housing, through the constraints and time lags of the construction process, to eventual delivery and depreciation. The output of the land use module at each timestep is the spatial distribution of residential and workplace locations, which links the land use module back to the transport module.

5 The case of Luxembourg

In this section, we present the application of the model through a case study of Luxembourg. Section 5.1 introduces the main characteristics of the study area and the model setup. The key assumptions and data are explained in Section 5.2. Section 5.3 discusses the model calibration and parameters. The results and model fit are presented and analysed in Section 5.4, with example policy scenarios explored in Section 5.5.

5.1 Case study area

The area of study in this application is the Greater Region of Luxembourg. Luxembourg is a small country with a total area of 2'586 km^2, bordered by Germany, Belgium, and France. Its dynamic economy attracts approximately 200'000 cross-border workers everyday from the neighbouring countries, accounting for nearly half of the national workforce. This substantial volume of daily commuting highlights the strong interconnection between Luxembourg and its cross-border regions, particularly in terms of both daily and residential mobility. Accordingly, the study area includes the Grand-Duchy of Luxembourg and the bordering territories of the neighbouring countries in Germany (Saarland and Rhineland-Palatinate), Belgium (Wallonia), and France (Lorraine). The cross-border areas are at border proximity territories defined based on the proximity zones identified in Luxembourg's national spatial planning strategy (PDAT) (Ministère de l'Aménagement du Territoire, 2023). The cross-border functional area of Luxembourg is illustrated in Figure 8. The Grand Duchy of Luxembourg is divided into 12 cantons, which serve as its administrative districts, as presented in Figure 9. For the analysis, each of these 12 internal cantons is taken as a zone. In addition, each bordering cross-border region in France, Belgium, and Germany is represented as a single aggregated zone, resulting in a total of 15 zones in the model.

Luxembourg has experienced remarkable economic prosperity in recent decades, emerging as one of the most prosperous countries in Europe. This growth has been accompanied by rapid demographic change. The population has increased by 54% since 2000 reaching 672'000 person in 2024, driven by both international migration and strong labour demand. In response to its favourable economic climate, many companies have relocated to or opened offices in Luxembourg, which has led to a substantial rise in job opportunities. The growth in number of jobs has outpaced population growth in relative terms, with a job per resident ratio of 0.76 in 2023, reflecting the exceptional weight of the labour market relative to the national population (Observatoire du développement territorial, 2025). A large share of jobs is filled by cross-border commuters, whose numbers rose from approximately 105'000 in 2005 to 166'000 in 2019 —an increase of 37%. Today, cross-border workers represent more than 40% of total employment, a proportion that has steadily grown over the past decade.

Figure 8: Map of greater region of Luxembourg; Luxembourg's cross-border functional area (Adapted from Ministère de l'Aménagement du Territoire (2023)).

In 2023, Luxembourg recorded 499'985 jobs, of which only 265'000 were held by residents, meaning 47% of the workforce lived in neighbouring countries, 43% of whom come from France, and almost equally from Germany and Belgium. This marks a dramatic shift from just 3% in 1961, highlighting the continued and growing dependence on cross-border labour (Observatoire du développement territorial, 2025). This puts pressure on transport networks, prompting each state to adjust its services to better meet user needs.

These combined trends reflect high levels of both residential and daily mobility, contributing to dynamic labour markets and population concentration in and around the country. A significant share of total employment is concentrated in Luxembourg City. This concentration of economic activity has placed strong pressure on the housing market, triggering a sharp rise in real estate prices not only in Luxembourg's urban core but also in its immediate surroundings. However, the housing supply has remained relatively inelastic, with limited new con-

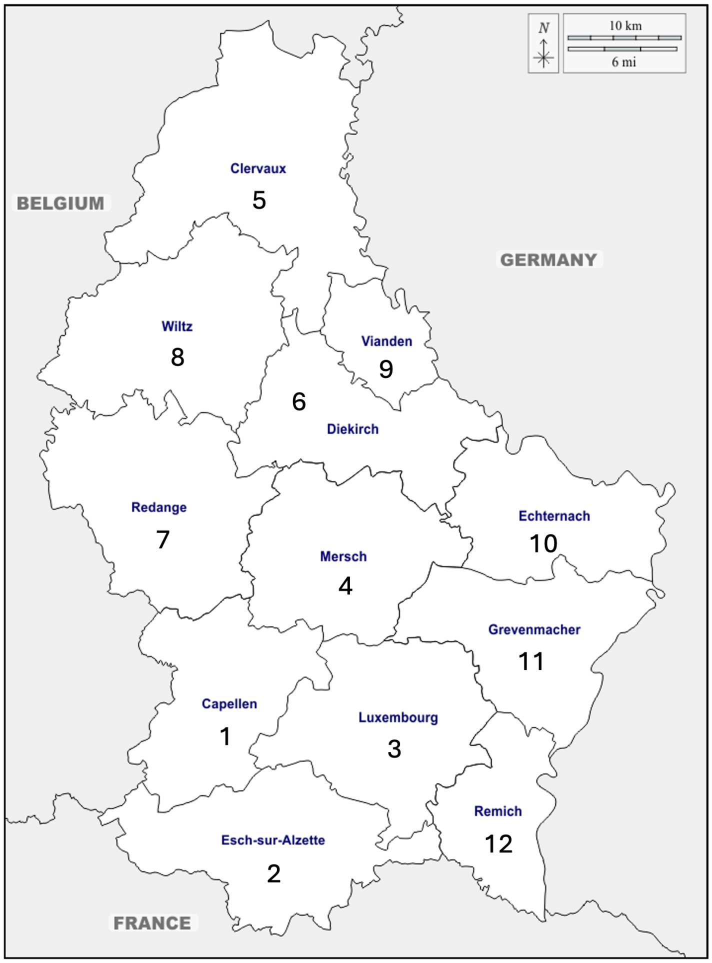

Figure 9: Plan of Luxembourg and its cantons

struction. This structural constraint has further intensified price growth and reduced accessibility to housing. As a result, households are pushed to relocate to suburban or neighbouring cross-border regions, reinforcing urban sprawl and increasing the need for daily travel. Empirical evidence shows that current urbanisation trends toward suburban and more remote peri-urban areas favour urban sprawl and car dependence. Although public transport has been free in Luxembourg since February 2020, this policy has not led to a significant reduction in car usage. The country continues to exhibit a high reliance on private vehicles, with 95% of households owning at least one car (MMUST, 2022). These developments have contributed to growing traffic congestion and complex interdependencies in spatial planning.

In light of these dynamics —marked by rapid population growth, cross-border labour dependence, housing pressure, and rising mobility demand— this case study adopts a systems thinking approach to model the complex interactions between population growth, residential mobility, and labour mobility within the greater region of Luxembourg. By capturing the spatial-temporal dimensions of urban change, we assess how housing, spatial planning, and mobility influence one another, and evaluate the impacts of policy measures and planning scenarios. The resulting tool enhances understanding of residential and mobility behaviours and provides a framework for projecting future trends in urban sprawl and population distribution. It supports decision-making by enabling stakeholders to assess the effects of different land use and transport policies , evaluate trade-offs, and align decisions with long-term territorial development objectives.

5.2 Data and key assumptions

This case study integrates data from multiple sources covering the period from 2001 to 2024, with temporal resolution varying from annual to decennial intervals, depending on data availability and collection frequency. Demographic data such as population counts, employment, and socio-demographic characteristics for Luxembourg are primarily obtained from national social security records. Corresponding data for the cross-border regions are collected from the respective national social security data of France, Belgium, and Germany. Information on commuting patterns and transport is derived from Luxembourg Mobility Observatory, including data from the 2001, 2011, and 2021 census datasets, as well as supplementary datasets on cross-border commuters. Housing and land use data such as housing surface, developments, land availability, rental prices, and urban densification are sourced from the Luxembourg Housing Observatory (Ministry of Housing and Spatial Planning, 2025) and the national population census. Due to the limited availability of detailed housing and land use data for the cross-border regions, simplified assumptions are applied to approximate these variables in the aggregated neighbouring zones.

The modelling time period is from 2001 for a period of 50 years. Daily timesteps are used in the model. As empirically observed, new immigrants to Luxembourg typically settle first in Luxembourg City. Accordingly, the model assumes that newly arrived immigrants choose the canton of Luxembourg as their initial place of residence. We assume that residents of Luxembourg work exclusively within the country and not in the cross-border regions. This is supported by MMUST (2022), which reports that only 1.5% work in neighbouring countries, a share sufficiently low to justify their exclusion from the model. Renting is assumed as the only means of satisfying housing demand.

In the transport demand model, the mode alternatives are car and public transport. All public transport is assumed to operate on an exclusive right-of-way; therefore, the proportion of public transport running in mixed traffic is zero, $\phi = 0$. Travel distances by car are computed as the distance between canton centroids, following a systematic approach based on official GIS data. The coordinates of each canton centroid in Luxembourg are derived from administrative boundary data provided by the Administration du Cadastre et de la Topographie (ACT) (Administration du Cadastre et de la Topographie, n.d.) via the Luxembourg open data portal. Centroids are calculated as the geometric center of each canton polygon in a GIS environment. For internal trips, average distances are estimated from canton surface areas, assuming trips are uniformly distributed within the zone. The average internal distance is approximated as the radius of a circle with an area equal to half the canton's area:

$$\bar{d}_{\text{int}} \approx \sqrt{\frac{S_z}{2\pi}} \tag{29}$$

where $\bar{d}_{\text{int}}$ denotes the average travel distance for intra-zonal commutes (origin and destination within the same zone), and S_z is the surface area of zone z.

In the three cross-border zones, simplifying assumptions are adopted due to data limitations. For the cross-border commuters, commute distances are estimated using the average home-to-work distances reported for employed persons Observatoire du développement territorial (2025). Rental prices in the cross-border regions are treated as exogenous, set to observed historical values and projected forward using an assumed growth rate, as these regions lie outside Luxembourg's planning boundary and their housing dynamics depend on factors other than cross-commuting. Furthermore, population dynamics in these zones are governed not only by endogenous move-in and move-out rates, but also by an exogenous migration component. This component captures in-migration from areas beyond the model boundaries into the cross-border regions and is estimated using annual population time series from the statistical institutes of the neighbouring countries. Moreover, in cross-border regions, only the share of residents who commute across the border is considered when estimating the pool of potential residential movers.

The model does not account for freight transport, route choice, general economic development, or population ageing processes. Car ownership and parking availability and pricing are not considered in the model. The case study is implemented in Vensim Personal Learning Edition (PLE) (Ventana Systems, 2025), a free version of the Vensim software designed for designing, modelling, and analysing system dynamics models.

5.3 Model parameters and calibration

Calibrating system dynamics models is inherently complex due to the high number of parameters, the interplay among variables, nonlinear feedback structures, data limitations, and the added challenge of the system being dynamic (Walker and Wakeland, 2011). According to Barlas (1996), feedback loops and time delays complicate calibration and the establishment of model fit, making the process both technically and conceptually demanding. Changes in one part of the model affect the other parts. This is a significant challenge in the calibration of the model due to its large size and its many relevant outputs.

The calibration of the model is carried out through an iterative, partly manual process. Parameter values are adjusted incrementally through trial-and-error. Empirical comparisons between model outputs and historical data are central to this process, guided by aggregated performance metrics. Calibration follows a sequential improvement approach, in which changes are introduced step by step and their effects on model outputs are monitored to reproduce the observed variables in the historical data as closely as possible. To reduce the endless loops of adjustments that can arise when calibrating a complex model, individual submodels are first calibrated in isolation before integrating them into the full framework. This involves building standalone versions of submodels to test key control logic before addressing the ensemble model. It is notable that while most system dynamics models are not primarily intended to produce point forecasts, reproducing historic trends increases model credibility.

The model is initialised with data from 2001, which serves as the base year. The model was then run dynamically from 2001 to 2024. Through an iterative process, the parameters are adjusted to match the population, rent prices, housing surface, and transport modal shares as close as possible. Model performance is evaluated by comparing modelled and observed values using indicators such as absolute relative deviation (Equation 30), mean percentage error (MPE) (Equation 31), and root mean squared error (RMSE) (Equation 32), with their formulas given below. $y_{\text{obs}}(t)$ denotes the observed value of the variable at time t, and $y_{\text{pred}}(t)$ is the modelled value at time t.

$$\text{Absolute Relative Deviation} = \frac{|y_{\text{pred}}(t) - y_{\text{obs}}(t)|}{|y_{\text{obs}}(t)|} \tag{30}$$

$$\text{MPE} = \frac{1}{T}\sum_{t=1}^{T}\frac{y_{\text{pred}}(t) - y_{\text{obs}}(t)}{y_{\text{obs}}(t)} \tag{31}$$

$$\text{RMSE} = \sqrt{\frac{1}{T}\sum_{t=1}^{T}\left(y_{\text{pred}}(t) - y_{\text{obs}}(t)\right)^2} \tag{32}$$

We employ estimation techniques for model parameters wherever possible with the data available to us. The parameters of the money-metric utility of generalised cost, $GC_{ij}(t)$ in Equation 4, are estimated by maximum likelihood using transport data from 2001. In the gravity model for trip distribution, the impedance parameter β_{GC}, in the deterrence function in Equation 4 is estimated with the Hyman method (Hyman, 1969), based on 2001 transport data. The Hyman method is an iterative calibration procedure that adjusts β_{GC} until the modelled travel flows matches the observed travel flows, using interpolation between successive estimates to accelerate convergence.

The parameters of the model for the case study, calibrated to the existing data or derived from consensus values in the empirical literature, are summarised in Table 2.

Table 2: Values and sources of parameters in the case study model.

Variable	Description	Unit	Value	Comment
$\lambda_{\text{trip}}^{\text{peak}}$	Average commute rate per employed individual during morning peak.	-	0.6	-
$\lambda_i^{\text{Empl}}(t)$	Employment rate in zone i.	-	$\lambda_i^{\text{Empl}}(t) \in [0, 1]$.	Based on population census.
$\lambda_i^{\text{WorkAge}}(t)$	Ratio of working age population in zone i.	-	$\lambda_i^{\text{WorkAge}}(t) \in [0, 1]$.	Based on population census.
β_{GC}	Impedance parameter.	1/Euro	0.154	Estimated using Hyman method.
μ	Scale parameter	-	1	Normalised to 1 as in linear-in-parameters utility specification.
$\beta_{\text{TT}}^{\text{GC}}$	Parameter of travel time in generalised cost.	Euro/Min	-0.634	Estimated with maximum likelihood estimation.
$\beta_{\text{TC}}^{\text{GC}}$	Parameter of travel cost in generalised cost.	-	-1	Normalisation for money-metric utility formulation.
$\beta_{\text{TC}}^{\text{car}}$, $\beta_{\text{TC}}^{\text{PT}}$	Parameter travel time by car/public transport.	1/Euro	-0.18	Estimated using maximum likelihood estimation.
$\beta_{\text{TT}}^{\text{car}}$, $\beta_{\text{TT}}^{\text{PT}}$	Parameter travel time by car/public transport.	1/Min	-0.12	Estimated using maximum likelihood estimation.
α	Scaling parameter in BPR relationship.	-	0.15	Based on California Department of Transportation (2022).
β	Shape parameter in BPR relationship.	-	4	Based on California Department of Transportation (2022).
Occ^{PC}	Car occupancy.	Person/Veh	1.16 for Luxembourg residents, 1.22 for cross-border workers.	Luxmobil survey 2017 (Ministere du Developpment durable et des Infrastructures, 2017).
$\eta_f(t)$	Fuel consumption.	liter/100km	A value between 6.15 and 8.5.	Based on data on fuel consumption of cars (Odysse Muree, 2024; International Energy Agency, 2021).

(Continued from previous page)

Variable	Description	Unit	Value	Comment
$p^{fuel}(t)$	Fuel price.	Euro/liter	A value between 0.75 and 1.56.	Based on historical data on fuel price from Luxembourg national statistics (Statista Research Department, 2025; Rhinocarhire.com, 2025).
$\kappa^{maint}(t)$	Operating cost per kilometer.	Euro/km	A value between 0.37 to 0.5.	Based on Markus Maibach et al. (2006).
$p^{toll}(t)$	Toll fees.	Euro	0	Luxembourg motorways are toll free (Wikipedia contributors, 2025).
$TC_{ij}^{PT}(t)$	Travel cost of public transport.	Euro	Before 2020: 2 Euro (Luxembourg residents), 7 Euro (cross-border commuters); After 2020: Free (Luxembourg residents), 5 Euro (cross-border commuters).	Based on Luxembourg public transport website (Mobilitéit, 2025).
θ^{PC}	Road demand surge threshold.	-	0.25	-
θ^{PT}	Public transport demand surge threshold.	-	0.25	-
$v_{ij}^{\theta,PC}$	Threshold speed car.	km/hr	30 km/hr for local roads and 55 km/hr for inter-cantonal roads.	Selected as a decision criterion considering information on average speed at morning rush hour on road and motorways in Luxembourg (RTL Today, 2023b,a).
β_{TT}^{Acc}	Parameter travel time in accessibility.	1/Min	-0.123	Calibrated to model fit.
$\Delta t_{perc,transp}$	Perception time of travel cost and time.	Day	60	-

(Continued from previous page)

Variable	Description	Unit	Value	Comment
τ_{PC}^{Cnst}, τ_{PT}^{Cnst}	Road/public transport infrastructure construction duration.	Year	3 years for local roads and 10 years for motorways.	Based on project timeline from planning to inauguration by Deputy Prime Minister of Luxembourg (Ministry of Mobility and Public Works (MMTP), Department of Mobility and Transport, 2022).
$\Delta t_{dec,transp}$	Time window within which transport demand changes are perceived for capacity expansion decision-making.	Day	730	-
τ_i^{mv}	Average residence time in zone i.	Day	A value between 3600 to 4500 days.	Based on data from Housing Observatory.
β_{Rent}	Parameter of rent price in residential location choice.	$m^2 \cdot$ Month/Euro	-0.3	Calibrated to model fit.
β_{Acc}	Parameter of accessibility in residential location choice.	-	0.9	Calibrated to model fit.
$\Delta t_{perc,Res}$	Perception time of rent and accessibility changes.	Day	90	-
$S_i^{per,norm}$	Normative residential surface area per person.	m^2/Person	Domicile surface area per person in the corresponding zone in base year 2001.	Based on data from Housing observatory data.
τ_{Rent}^{adj}	Time to adjust rent price.	Day	365	-
Φ	Elasticity of housing supply to rent price.	-	0.02	Based on Dautel et al. (2024).
τ_{Res}^{Cnst}	Residential construction duration.	Day	720	-
τ_{Res}^{life}	Average building lifetime.	Year	100	-
$\Delta t_{dec,Res}$	Time window within which housing construction and rent price changes are perceived for decision-making.	Day	365	-

5.4 Results and analysis: Base scenario and model assessment

Using the calibrated model, population dynamics are modelled from 2001 to 2024. Figure 10 presents the number of residents in each zone over this period. According to the model results, the population of the Grand-Duchy of Luxembourg increase by 228’160 persons, or 52%, between 2001 and 2024. Among the internal cantons of Luxembourg, the largest absolute increases occur in zone 3 (canton of Luxembourg) with +62’197 persons, zone 2 (canton of Esch-sur-Alzette) with +44'539, and zone 1 (canton of Capellen) with +20'970 persons. This can be explained with their higher accessibility and the concentration of jobs -more than 70% of national employment is located in these zones, particularly in zones 2 and 3— which makes them attractive despite their higher rent prices. Zone 3 in particular shows the strongest population growth as newcomers to Luxembourg tend to settle first in central zone 3, the canton of Luxembourg.

Meanwhile, the population in the cross-border regions appears relatively stable. The strongest increase is in the Belgian cross-border zone, with growth of about 10%, or +348'000 persons, between 2001 and 2024. In the plot, this apparent stability can be explained by the much larger population base of the cross-border regions, in the order of millions, compared to country of Luxembourg, which has a population in the hundreds of thousands. The entire country of Luxembourg has only about 670'000 residents in 2024, so changes of just a few thousand people in individual cantons already appear as visible shifts in the curves.

The model results are compared with observed data to evaluate the model fit. Figure 10 provides a visual comparison of the observed and modelled number of residents by zone in the Greater Region of Luxembourg, illustrating the overall agreement of modelled results with the data. To quantify the model fit, we compute performance indicators for the period 2001–2024. Statistical measures —absolute relative deviation (Equation 30), mean percentage error (MPE, Equation 31), and root mean squared error (RMSE, Equation 32) between modelled and data— are reported in Table 3, quantifying the deviation between modelled and observed number of residents by zone. The model shows a reasonable fit across Luxembourg's zones, with maximum absolute relative deviations mostly below 0.15, except in zones 5 and 8. Errors are generally larger for Luxembourg's internal zones (higher RMSE values) compared to the cross-border regions, where deviations remain very small. This can be attributed to the population structure of the cross-border zones: while the plots show their entire resident population, only a small fraction of these residents —less than 8%— are commuters to Luxembourg and thus eligible for residential relocation in our framework. As a result, the potential relocating population from these zones is very limited, which keeps deviations small.

Similarly, Figure 11 presents the modelled and observed rent price, while Table 4 summarises the corresponding performance indicators for 2001-2024. The results indicate an overall reasonable fit, with median absolute relative deviations mostly below 0.2. Larger deviations appear in some zones, most notably in zone 5. Across most zones, Figure 11 shows a systematic underestimation of rent prices, with mean percentage errors (MPE) generally below 15%. This underestimation stems from the residential development sub-model, which tends to overestimate new construction volumes (Table 5), thereby reducing market tightness and lowering the modelled rents. Overall, the model captures the general spatial variation in rent prices but consistently underestimates their magnitude.

For the transport sub-model, we have only three data points from census years 2001, 2011, and 2021. The share of car commutes from the model results is compared with the corresponding shares computed from the data. Table 6 summarises the modelled and observed modal shares of car for these years. Overall, the data confirm that the modal split is dominated by cars. The model consistently underestimates car use, with moderate deviations in 2001 but a much stronger underestimation in 2011 and 2021. This suggests that the model does not fully capture changes in commuting behaviour or influencing factors. Addressing these discrepancies require further investigation into the determinants of commuting behaviour, supported by access to disaggregate census and mobility survey data. In addition, testing different coefficient parameters for the BPR-type speed–flow relationship (Equation 8), as recommended in transport modelling manuals, could improve the calibration of congestion effects, which influence mode choice outcomes in the model.

Overall, the agreement between the model and observed data is satisfactory for a first implementation, confirming that the structural assessment of the model is correct and providing a solid foundation for further refinements to improve the model fit.

Table 3: Performance indicators for modelled number of residents versus observed data from 2001 to 2024 in Greater region of Luxembourg.

Zone	**Absolute Relative Deviation**				**MPE**	**RMSE**
	Sum	**Max**	**Standard deviation**	**Median**		
1	301.10	0.079	0.021	0.035	-0.007	1939.20
2	453.61	0.12	0.041	0.055	-0.052	11943.14
3	287.33	0.091	0.025	0.027	-0.0074	7724.57
4	238.18	0.079	0.019	0.022	-0.0097	1078.30
5	1058.9	0.30	0.091	0.104	0.050	2934.22
6	351.95	0.13	0.035	0.027	0.030	1858.73
7	457.17	0.10	0.034	0.051	-0.048	1016.67
8	944.73	0.21	0.080	0.14	0.11	2313.86
9	642.71	0.14	0.046	0.071	0.044	464.87
10	725.83	0.14	0.043	0.097	-0.043	1626.09
11	245.37	0.085	0.022	0.028	0.027	1055.26
12	383.10	0.098	0.028	0.045	-0.012	1097.48
Belgium	7.86	0.0015	0.0005	0.00108	0.00083	3815.37
Germany	5.97	0.003	0.00075	0.00058	0.00071	5250.77
France	23.20	0.0045	0.0015	0.0028	0.0027	5592.43

Table 4: Performance indicators for modelled rent price versus observed data from 2001 to 2024 in Grand Duchy of Luxembourg.

Zone	**Absolute Relative Deviation**				**MPE**	**RMSE**
	Sum	**Max**	**Standard deviation**	**Median**		
1	724.92	0.13	0.035	0.09	-0.086	1.57
2	341.77	0.16	0.038	0.030	-0.037	1.11
3	689.37	0.23	0.040	0.082	-0.082	2.24
4	775.30	0.24	0.061	0.088	-0.092	1.92
5	1830.87	0.36	0.11	0.25	-0.21	3.15
6	1090.17	0.27	0.058	0.13	-0.12	2.09
7	1308.15	0.26	0.063	0.18	-0.15	2.20
8	1092.80	0.21	0.051	0.13	-0.13	1.70
9	1193.77	0.25	0.057	0.14	-0.14	1.91
10	1244.02	0.29	0.072	0.16	-0.14	2.30
11	945.34	0.20	0.049	0.11	-0.11	1.95
12	1368.96	0.21	0.053	0.18	-0.16	2.58

Table 5: Relative deviation (%) of housing surface between model results and data in Grand Duchy of Luxembourg.

Zone	**2011**	**2021**
1	8.37%	8.66%
2	5.93%	4.54%
3	3.66%	6.88%
4	8.50%	7.56%
5	11.70%	17.63%
6	7.74%	10.78%
7	34.69%	30.75%
8	15.27%	16.02%
9	7.80%	12.47%
10	4.95%	8.02%
11	5.24%	7.28%
12	5.08%	7.23%

Table 6: Share of car commutes in model results and data.

Year	**Model**	**Data**	**Deviation**
2001	0.60	0.72	-0.12
2011	0.52	0.72	-0.20
2021	0.43	0.68	-0.25

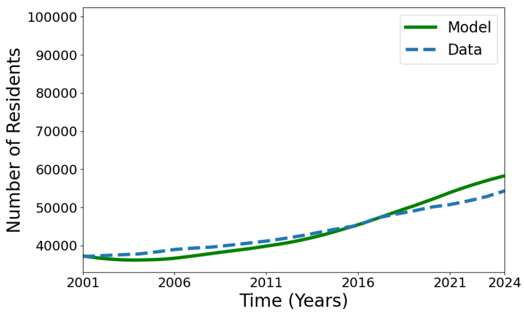

(a) Residents zone 1

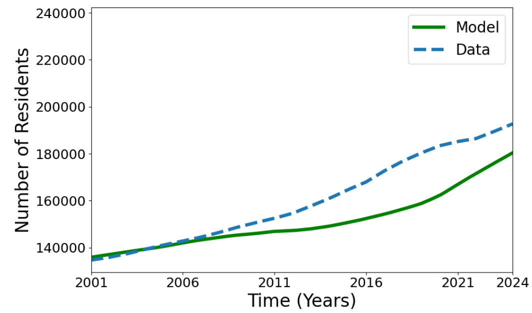

(b) Residents zone 2

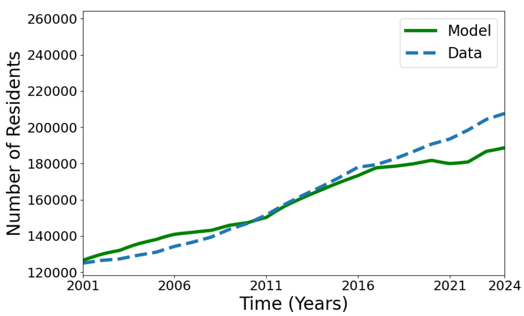

(c) Residents zone 3

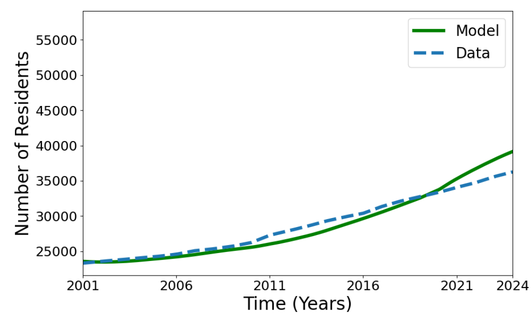

(d) Residents zone 4

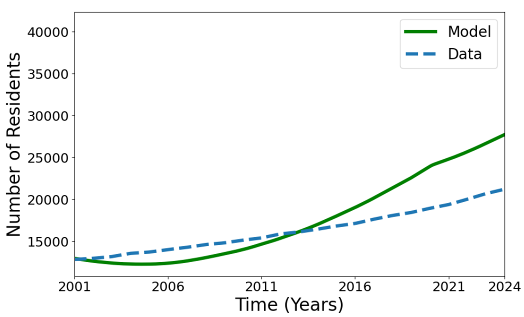

(e) Residents zone 5

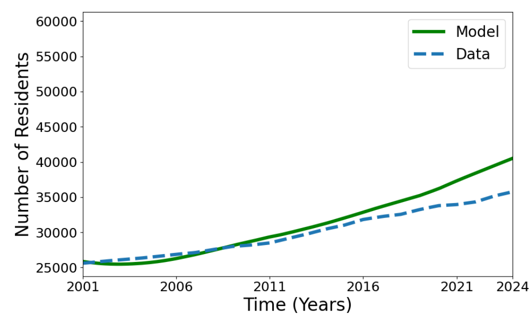

(f) Residents zone 6

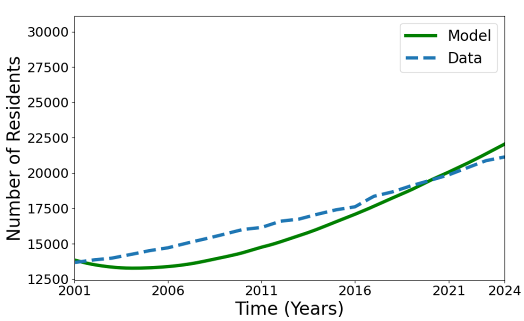

(g) Residents zone 7

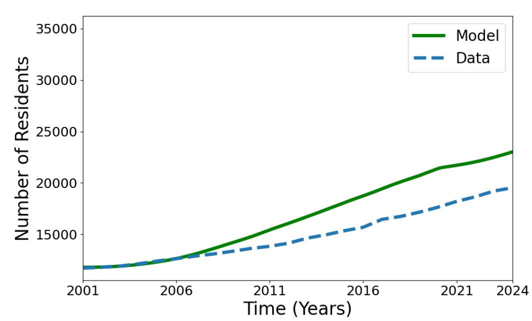

(h) Residents zone 8

Figure 10: Number of residents by zone in the Greater Region of Luxembourg - Continued.

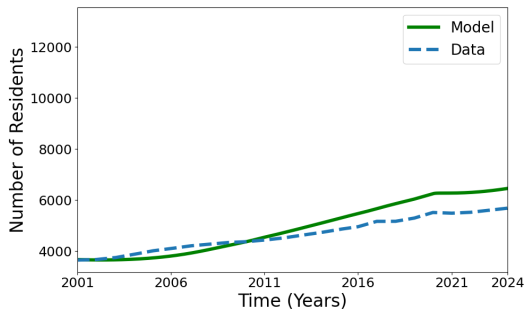

(i) Residents zone 9

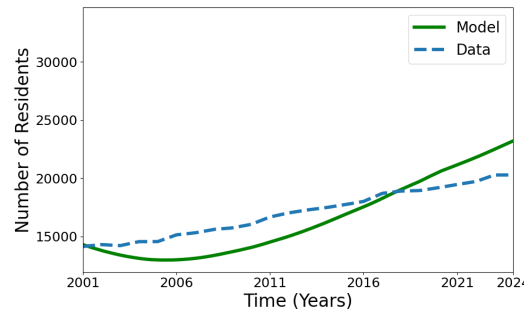

(j) Residents zone 10

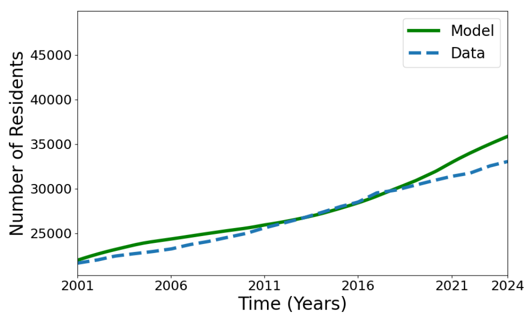

(k) Residents zone 11

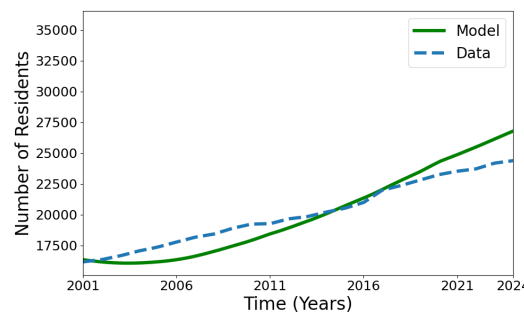

(l) Residents zone 12

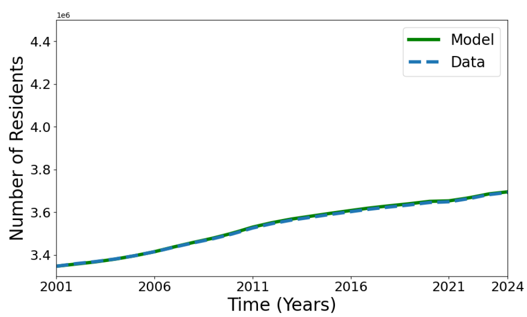

(m) Residents cross-border Belgium

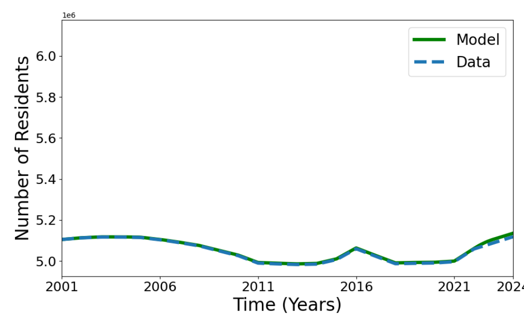

(n) Residents cross-border Germany

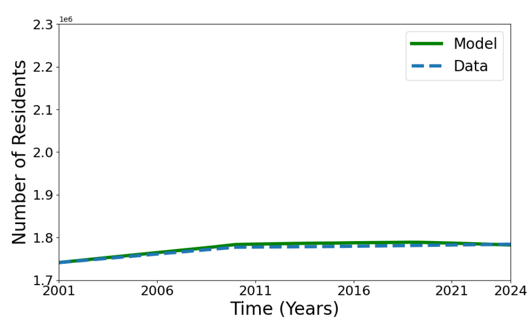

(o) Residents cross-border France

Figure 10: Number of residents by zone in the Greater Region of Luxembourg.

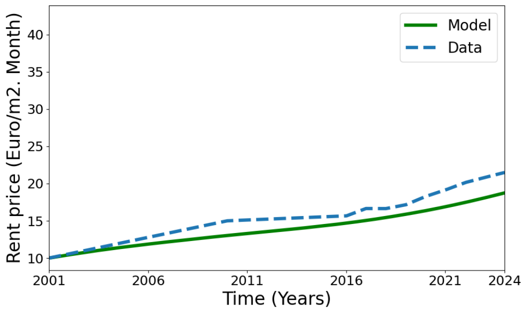

(a) Rent price zone 1

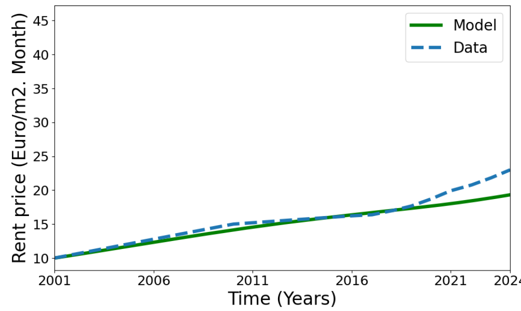

(b) Rent price zone 2

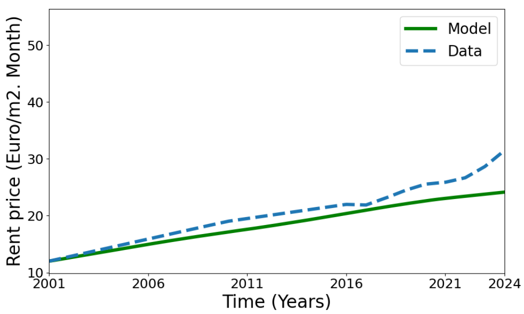

(c) Rent price zone 3

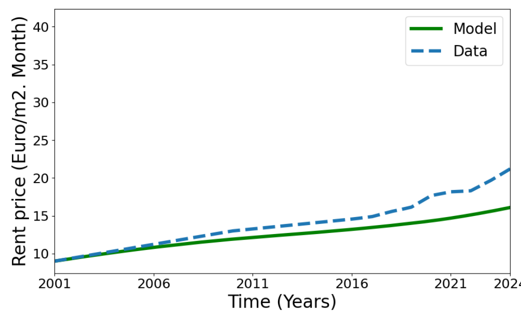

(d) Rent price zone 4

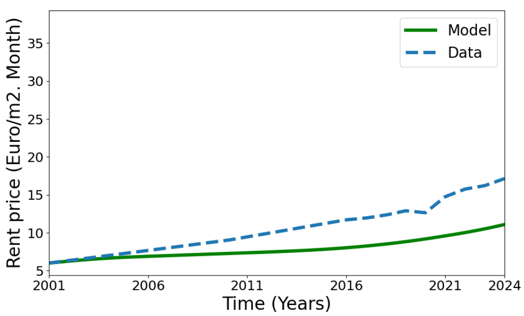

(e) Rent price zone 5

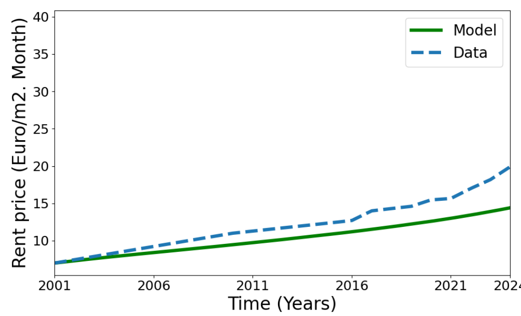

(f) Rent price zone 6

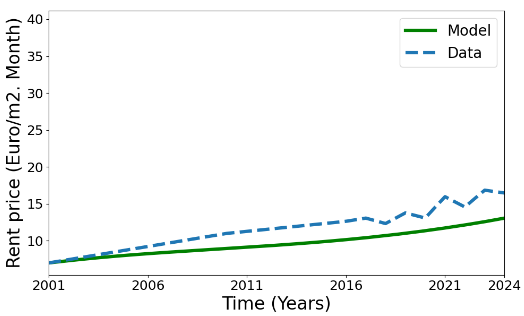

(g) Rent price zone 7

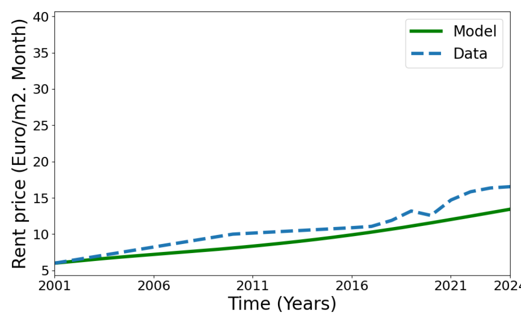

(h) Rent price zone 8

Figure 11: Monthly rent price per square meter by zone in Grand Duchy of Luxembourg - Continued.

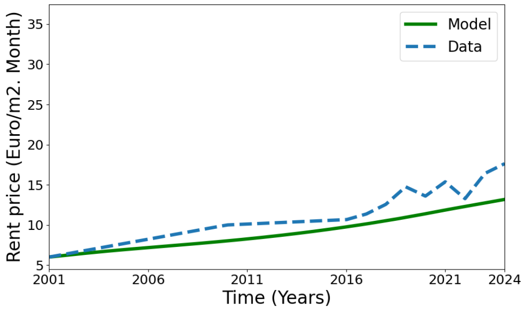

(i) Rent price zone 9

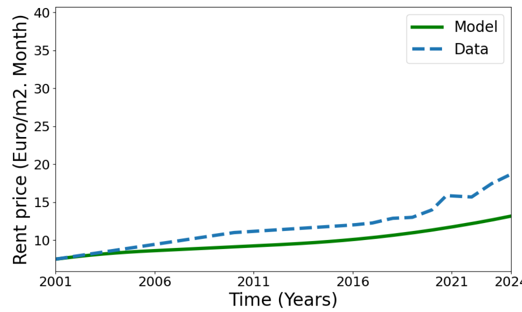

(j) Rent price zone 10

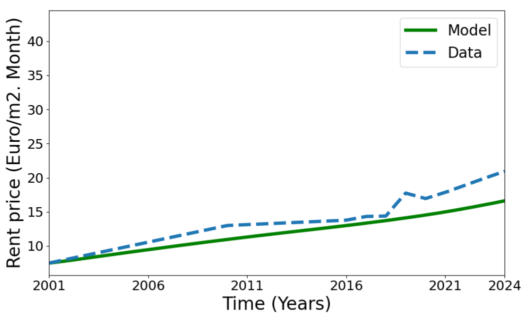

(k) Rent price zone 11

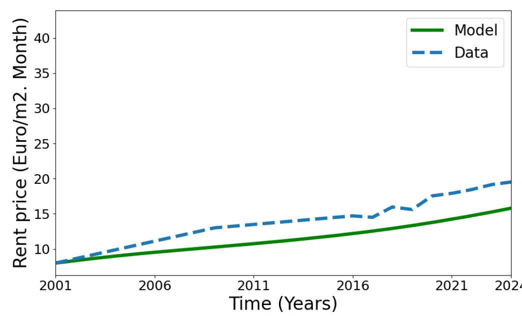

(l) Rent price zone 12

Figure 11: Monthly rent price per square meter by zone in Grand Duchy of Luxembourg.

5.5 Policy and scenario analysis

In this section, we present model results under example counterfactual scenarios and policies over a time horizon from 2001 to 2051, to analyse their impact on distribution of residents in cantons of Grand Duchy of Luxembourg. For the demographic and economic projections, we use the guidelines of National Institute of Statistics and Economic Studies of Luxembourg (STATEC), following its intermediate growth scenario, which assumes annual GDP growth of 3% and provide demographic projections for 2030 and 2060 (Statec, 2017). Key demographic changes include the number of additional residents, jobs, and cross-border workers. The net annual birth rate is projected at 2'978 person per year until 2030, declining to 793 person per year until 2060. Until 2030, 10'000 foreign workers are expected to be attracted each year, equally split between cross-border commuters and active immigrants (5'000 person each). Accounting for inactive immigrants, the net annual migration is projected at 10'080 persons until 2030, and 10'313 persons thereafter. By 2030, the number of jobs in Luxembourg will reach 570'000, comprising 268'000 cross-border workers and 302'000 resident workers. By 2051, total employment will rise to 726'000, with 374'000 cross-border workers and 352'000 resident workers. The relative distribution of jobs across the cantons of Luxembourg is assumed to follow the proportions observed in the latest census in 2021. For the 2001–2051 model, these demographic changes are used as exogenous demographic drivers, while the model endogenously propagates the population across different zones.

The framework allows us to identify the start and end points, as well as the initial and final levels of any policy instrument. It also enables the specification of combination policies by implementing multiple policy instruments simultaneously. The following scenarios presented are illustrative examples, intended to demonstrate the model's capabilities and application, and are not a comprehensive exploration or evaluation of alternative policies to determine the most effective means of achieving specific objectives. As in most prospective research, the scenarios are what-if cases meant to spark discussion about possible futures, not absolute predictions.

5.5.1 Construction of affordable housing

A plausible policy scenario is the construction of affordable housing in different cantons of Luxembourg. In our analysis, affordable housing refers to dwellings provided through public or subsidised schemes, available to all households and rented at a price lower than the average rent of the zone at the time. In reality, the concept in Luxembourg is more specific: it designates publicly or subsidised dwellings offered for rent or purchase at prices linked to household income and composition, allocated through legal eligibility criteria to ensure that modest-income residents can secure adequate housing without exceeding a reasonable share of their budget (Ville de Luxembourg, 2025). Since our model does not account for income groups and considers renting as the sole means of meeting housing demand, we apply a simplified definition in which affordable housing is available to all and exclusively offered for rent at below-average zone prices.

The scenario analysis is defined as follows. We assume a construction shock of 150'000 square meters of affordable housing, completed in 2030. This construction volume is applied consistently across different regions of Luxembourg. We denote the scenario involving the construction in zone i as AFFORDCONSTR_i. Figure 12 presents the evolution of residents by zone for selected scenarios as examples: (i) construction of affordabe housing in zone 1 (AFFORDCONSTR_1), (ii) construction of affordabe housing in zone 3 (AFFORDCONSTR_3), and (iii) construction of affordabe housing in zone 9 (AFFORDCONSTR_9), The base scenario serves as the reference for evaluating the effects of the tested policies. Table 7 reports the percentage deviation in population across the zones of Grand Duchy of Luxembourg relative to the baseline scenario, under the affordable housing construction policies, for the period following policy implementation (2030–2051). Table 8 summarises the corresponding absolute deviations in the number of residents by zone.

Assuming uniform construction costs nationwide, an equal investment yields varying population effects across zones. As expected, building affordable housing in a given zone increases that zone's population, while other zones experience a small decrease or no change at all. The relative effect is more pronounced in smaller, less developed zones; for instance, constructing affordable housing in zone 9 can produce a maximum population increase of 65% and an average population 30% higher than in the baseline scenario. In absolute terms, however, construction in zones with better accessibility and stronger job markets produces larger population gains. For example, the same level of investment results in an average population increase of 34'400 residents in the central zone 3, compared to 3'700 additional residents in the less developed zone 9 over time period of 2030-2051.

Following the construction shock, the initial population surge gradually tapers toward baseline levels without falling below them, due to reduced accessibility from traffic congestion and higher rents driven by market pressure from the earlier growth. Nonetheless, the overall population trend in the zone with housing construction remains upward between 2030 and 2051. In the long term, constructing housing while controlling rent prices appears to be an effective strategy for attracting and retaining residents in a zone. It is also notable that accounting for income groups and latent proxies of neighbourhood quality within the model could further influence these dynamics, which can be explored in future extensions.

Table 7: Percentage change in zone population relative to baseline under affordable housing policy scenarios (AffordConstr_i) for the period 2030-2051.

Scenario / Zone	AffordConstr_1			AffordConstr_2			AffordConstr_3			AffordConstr_4		
Zone	**Max**	**Min**	**Average**	**Max**	**Min**	**Average**	**Max**	**Min**	**Average**	**Max**	**Min**	**Average**
1	31%	0%	17%	4%	-10%	-3%	3%	-9%	-3%	1%	-2%	-1%
2	1%	-3%	-1%	27%	0%	15%	2%	-7%	-2%	1%	-2%	0%
3	1%	-2%	-1%	3%	-6%	-2%	29%	0%	14%	1%	-1%	-1%
4	1%	-3%	-1%	2%	-7%	-3%	2%	-6%	-3%	33%	0%	19%
5	2%	-4%	-1%	4%	-10%	-3%	5%	-9%	-3%	2%	-2%	-1%
6	2%	-3%	-1%	3%	-8%	-3%	3%	-7%	-3%	2%	-2%	-1%
7	2%	-3%	-1%	4%	-9%	-3%	3%	-7%	-3%	2%	-2%	-1%
8	3%	-4%	-1%	5%	-10%	-2%	4%	-9%	-3%	2%	-2%	-1%
9	4%	-5%	0%	7%	-11%	-2%	6%	-10%	-2%	3%	-3%	-1%
10	2%	-4%	-1%	5%	-9%	-2%	4%	-8%	-2%	2%	-2%	-1%
11	1%	-3%	-1%	3%	-7%	-2%	2%	-7%	-3%	1%	-2%	-1%
12	2%	-3%	-1%	4%	-8%	-2%	3%	-8%	-2%	2%	-2%	-1%

Scenario / Zone	AffordConstr_5			AffordConstr_6			AffordConstr_7			AffordConstr_8		
Zone	**Max**	**Min**	**Average**	**Max**	**Min**	**Average**	**Max**	**Min**	**Average**	**Max**	**Min**	**Average**
1	1%	-2%	0%	1%	-2%	-1%	1%	-1%	0%	1%	-2%	0%
2	1%	-2%	0%	1%	-2%	0%	1%	-1%	0%	1%	-1%	0%
3	1%	-1%	0%	1%	-2%	0%	1%	-1%	0%	1%	-1%	0%
4	1%	-2%	0%	1%	-2%	-1%	1%	-1%	0%	1%	-1%	0%
5	42%	0%	18%	3%	-3%	0%	1%	-2%	0%	1%	-2%	0%
6	1%	-2%	0%	34%	0%	18%	1%	-1%	0%	1%	-2%	0%
7	1%	-2%	0%	2%	-2%	-1%	36%	0%	20%	1%	-2%	0%
8	2%	-2%	0%	2%	-2%	-1%	0%	-1%	0%	41%	0%	20%
9	2%	-2%	0%	3%	-3%	0%	2%	-2%	0%	2%	-2%	0%
10	1%	-2%	0%	2%	-2%	-1%	1%	-1%	0%	1%	-2%	0%
11	1%	-2%	0%	1%	-2%	-1%	1%	-1%	0%	1%	-1%	0%
12	1%	-2%	0%	2%	-2%	-1%	1%	-1%	0%	1%	-2%	0%

Scenario / Zone	AffordConstr_9			AffordConstr_10			AffordConstr_11			AffordConstr_12		
Zone	**Max**	**Min**	**Average**	**Max**	**Min**	**Average**	**Max**	**Min**	**Average**	**Max**	**Min**	**Average**
1	1%	-1%	0%	1%	-1%	0%	1%	-2%	-1%	1%	-2%	0%
2	1%	-1%	0%	1%	-1%	0%	1%	-2%	0%	1%	-2%	0%
3	1%	-1%	0%	1%	-1%	0%	1%	-1%	0%	1%	-1%	0%
4	1%	-1%	0%	1%	-1%	0%	1%	-2%	-1%	1%	-1%	0%
5	1%	-1%	0%	1%	-2%	-1%	2%	-2%	-1%	1%	-2%	0%
6	1%	-1%	0%	1%	-1%	0%	1%	-2%	-1%	1%	-2%	0%
7	1%	-1%	0%	1%	-2%	0%	1%	-2%	-1%	1%	-2%	0%
8	0%	-1%	0%	1%	-2%	0%	2%	-2%	-1%	1%	-2%	0%
9	66%	0%	30%	2%	-2%	0%	2%	-3%	0%	2%	-2%	0%
10	1%	-1%	0%	42%	0%	21%	2%	-2%	-1%	1%	-2%	0%
11	1%	-1%	0%	1%	-1%	0%	36%	0%	20%	1%	-1%	0%
12	1%	-1%	0%	1%	-2%	0%	1%	-2%	0%	43%	0%	21%

Table 8: Absolute change in zone population relative to the baseline scenario under affordable housing policy scenarios (AFFORDCONSTR_i) for the period 2030-2051.

Zone \ Scenario	AFFORDCONSTR_1			AFFORDCONSTR_2			AFFORDCONSTR_3			AFFORDCONSTR_4		
	Max	**Min**	**Average**	**Max**	**Min**	**Average**	**Max**	**Min**	**Average**	**Max**	**Min**	**Average**
1	27587	0	15371.87	3705	-8230	-2474.93	3278	-7359.70	-2667.31	1268	-1701.20	-461.26
2	2702	-6515	-1585.02	62113	0	33903.14	3734	-14390	-4612.87	2647	-3986.00	-984.44
3	3146	-6150	-2106.77	6078	-15150	-5218.48	68112	0	34464.36	2480	-3636	-1329.56
4	759.90	-1395.50	-499.91	1368.40	-3351.60	-1282.78	1106.80	-2977	-1387.65	16688.80	0	9958.38
5	971.30	-1542.70	-352.84	1635.30	-3653.50	-907.66	1921.60	-3228.20	-925.09	923.50	-956.60	-208.77
6	1091.30	-1667.80	-551.68	2067.00	-3973.30	-1409.82	1720.40	-3517.10	-1547.74	923.40	-1023.60	-346.28
7	601.40	-922.90	-293.18	1188.20	-2210.60	-740.64	979.40	-1981.60	-807.27	487.10	-567.40	-184.91
8	955.30	-1321.20	-267.66	1916	-3135.80	-660.25	1564.60	-2815.70	-782	770.40	-808.30	-174.67
9	574.10	-564	-12.30	971.60	-1336.90	-175.77	798.20	-1180	-198.85	409.60	-343	11.85
10	773.60	-1104	-288.55	1550.20	-2594.70	-732.85	1288.50	-2390.60	-827.34	623.90	-680.90	-184.11
11	694.30	-1275.90	-383.68	1287.20	-3069.30	-978.23	1054	-2741	-1079.20	604.60	-777.10	-240.58
12	670.50	-1112.60	-251.75	1284.10	-2662.10	-636.70	1049	-2390.60	-742.12	572.40	-676.20	-160.75

Zone \ Scenario	AFFORDCONSTR_5			AFFORDCONSTR_6			AFFORDCONSTR_7			AFFORDCONSTR_8		
	Max	**Min**	**Average**	**Max**	**Min**	**Average**	**Max**	**Min**	**Average**	**Max**	**Min**	**Average**
1	948	-1511.20	-232.67	1221	-1846.50	-432.91	703	-953.70	-229.51	546	-1337.60	-267.23
2	2410	-3588	-501.76	2479	-4260	-922	1451	-2264	-498.02	1518	-3142	-574.53
3	2011	-3360	-872.51	2585	-3979	-1320.01	1467	-2139	-709.67	1449	-3043	-834.81
4	447.50	-764.50	-177.79	661.60	-921.90	-298.01	388.90	-485	-159.91	320.80	-654.80	-187.45
5	14847	0	6717.04	830.50	-1028.50	-207.20	492.70	-544.70	-108.03	375.90	-713.50	-142.77
6	652.30	-912.60	-188.16	17857.90	0	9870.13	530.30	-583.20	-177.02	462.40	-779.40	-200.65
7	365.50	-501.70	-104.14	495.50	-610.90	-177.03	9710.10	0	5503.67	264.20	-432.40	-108.52
8	679.70	-726.10	-73.49	781.50	-875.20	-157.43	435.80	-465.50	-85.63	13118.20	-1751.50	6709.02
9	392.30	-311.10	27.04	457	-373.10	17.98	235.30	-197.80	-12.10	278.30	-265.50	6.29
10	494	-603.50	-90.68	634.30	-733.80	-171.28	357.40	-388.80	-92.56	328	-515.80	-99.69
11	439.70	-698.30	-130.96	597.50	-841.80	-228.67	344.90	-444.80	-123.11	284	-600.50	-140.42
12	500.10	-609.70	-72.45	570.80	-733.50	-146.80	322.50	-389.10	-79.66	321	-526.80	-84.82

Zone \ Scenario	AFFORDCONSTR_9			AFFORDCONSTR_10			AFFORDCONSTR_11			AFFORDCONSTR_12		
	Max	**Min**	**Average**	**Max**	**Min**	**Average**	**Max**	**Min**	**Average**	**Max**	**Min**	**Average**
1	541	-779.60	-126.08	762	-1239.70	-263.24	1052	-1575.20	-392.66	704	-1387.90	-284.65
2	1259	-1909	-278.22	1564	-2933	-569.15	2118	-3648.80	-839.46	1526	-3253	-610.99
3	1218	-1801	-468.99	1735	-2778	-844.36	2208	-3464.40	-1155.95	1721	-3130	-891.63
4	303	-401.20	-96.23	430.20	-623.90	-186.65	580.20	-778.80	-266.73	411	-681.80	-199.86
5	350.50	-436.50	-67.44	494.10	-692.40	-132.08	708.30	-866.40	-184.11	405	-746.60	-147.12
6	417.10	-477.10	-103.86	599.60	-746.70	-203.64	790.40	-932.20	-294.86	574.20	-812.70	-215.25
7	226.60	-261.60	-57.37	326.10	-413.60	-110.32	423.60	-517.90	-157.99	318.90	-450.70	-116.44
8	370.70	-381.50	-43.56	504.30	-596.40	-93.06	650.40	-743.30	-142.61	490.50	-651	-94.42
9	8051.60	0	3746.32	300.70	-254.30	15.30	352.80	-316.30	9.37	297.10	-276.70	8.92
10	288	-314.80	-51.92	12378.40	0	6566.23	535.30	-620	-154.08	397.20	-538.40	-108.18
11	270.80	-366.40	-72.18	384.30	-571.40	-141.76	15381.40	0	8874.09	361.80	-625	-150.33
12	273.60	-320.40	-42	361.60	-500	-88.28	476.70	-623.60	-133.71	13568.10	0	7092.67

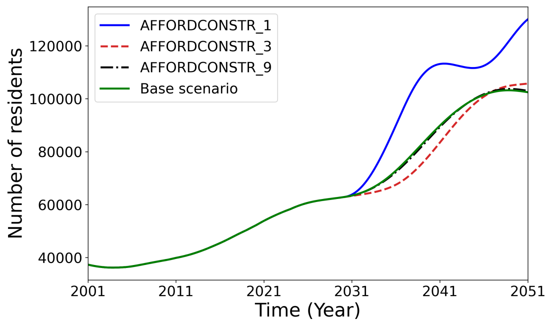

(a) Residents zone 1

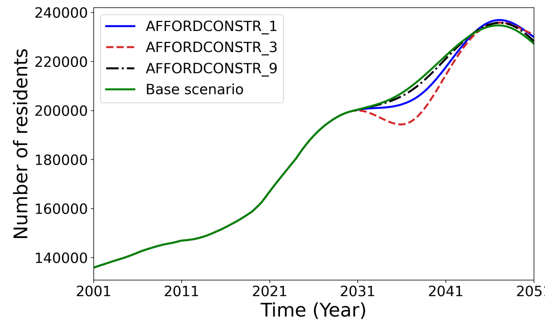

(b) Residents zone 2

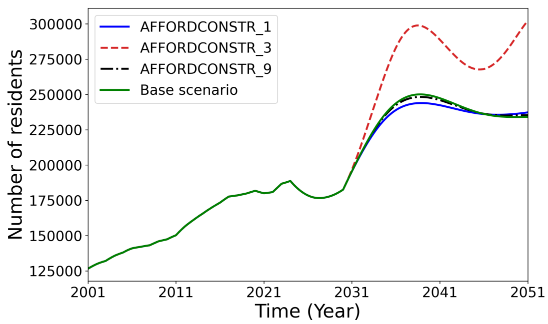

(c) Residents zone 3

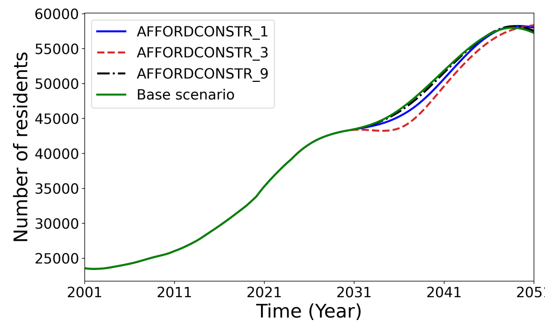

(d) Residents zone 4

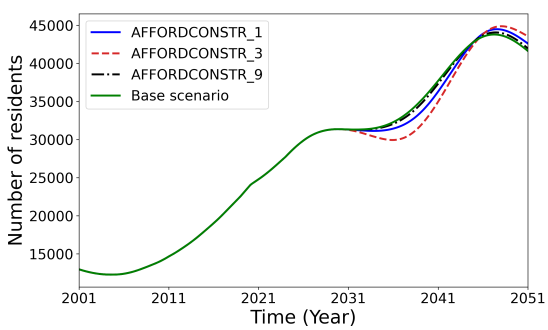

(e) Residents zone 5

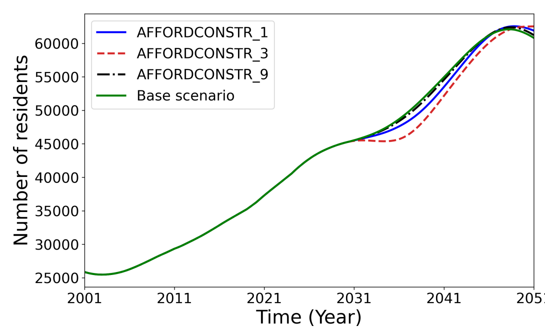

(f) Residents zone 6

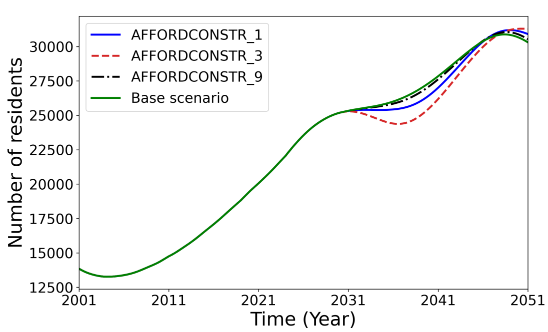

(g) Residents zone 7

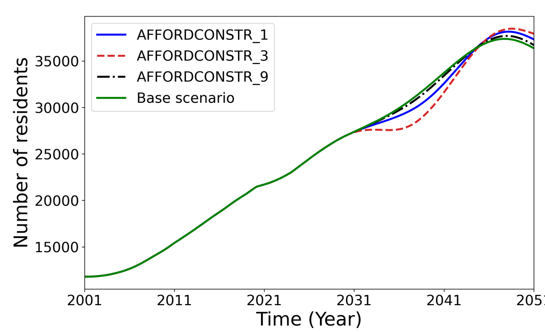

(h) Residents zone 8

Figure 12: Number of residents in each zone under affordable housing policies (AFFORDCONSTR_i) - Continued.

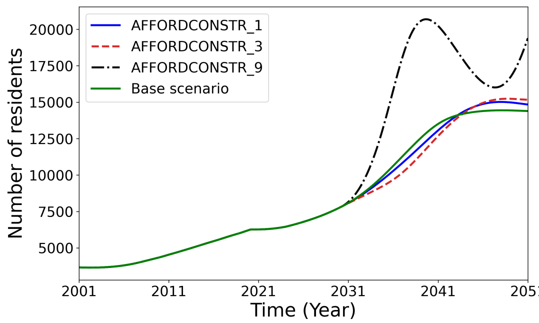

(i) Residents zone 9

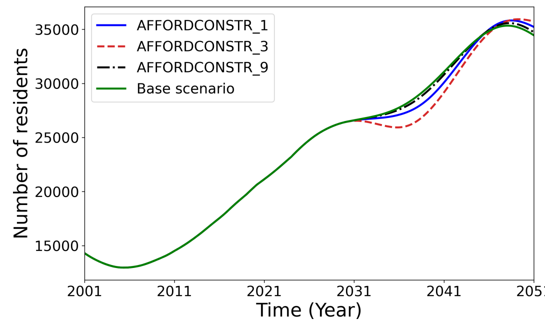

(j) Residents zone 10

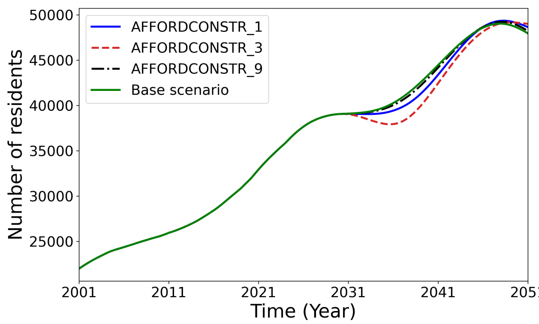

(k) Residents zone 11

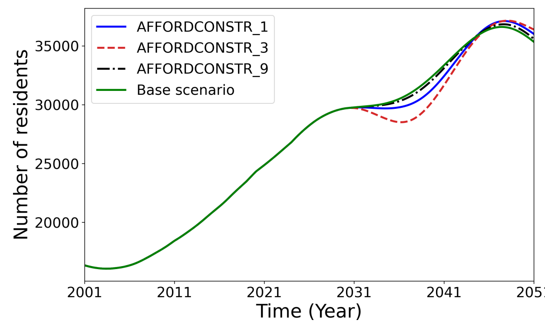

(l) Residents zone 12

Figure 12: Number of residents in each zone affordable housing policies (AFFORDCONSTR_i).

5.5.2 High speed tram between Luxembourg City and Esch-sur-Alzette

In this subsection we evaluate two policy scenarios. We model a policy scenario with a fast-tram link between the cantons of Luxembourg and Esch-sur-Alzette (zones 2 and 3) that opens in 2030, reducing travel time between these zones by 30%. We refer to this scenario as TRAM. We also test a combined policy case in which the fast tram is accompanied by a one-off addition of 60'000 square meters affordable housing in zone 3, available in 2030. We refer to this scenario as TRAM+HOUSE3. Figure 13 presents the evolution of residents by zone under both scenarios. The base scenario serve as the reference for evaluating the effects of the tested scenarios.

The TRAM scenario, initially increases the populations of zones 2 and 3. The new fast tram line between these zones boosts accessibility, enhancing their relative attractiveness and drawing more residents. Zone 3, as the central district with higher rents but abundant job opportunities, experiences a moderate population increase. Zone 2, a suburban area with lower rental prices and a solid though smaller job market, sees a more substantial average increase. This difference reflects the tendency of households to relocate farther from the central zone when improved transport connections allow convenient access, especially when rent prices are lower. As zones 2 and 3 already host about 60% of the country's population, the inflow toward them is mirrored by declines elsewhere. The increases, however, are temporary. Within about five years, rising demand drives up rents and induces more travel, which increases travel times and reduces accessibility. The subsequent decline in the populations of zones 2 and 3 is therefore driven by both higher rents from earlier growth pressures and reduced accessibility due to congestion. These effects prompt a gradual decrease in population, eventually returning toward —and in some cases falling below— baseline levels.

In TRAM+HOUSE3, the additional housing in zone 3 dampens and delays this decline: populations remain elevated for longer, and the subsequent drop is smaller. Overall, the results indicate that while fast transit can quickly shift residential patterns, maintaining these shifts over time requires adequate housing supply to ease market pressure and prevent rent escalation.

Table 9 summarises the percentage deviation in population across the zones of the Grand Duchy of Luxembourg, relative to the baseline scenario, under the fast-tram link (TRAM) and the combined tram and housing shock in zone 3 (TRAM+HOUSE3). The table reports the maximum and minimum percentage changes in population relative to the baseline, along with the average deviation over the period following policy implementation (2030–2051). In the TRAM scenario, the fast tram boosts the population in zones 2 and 3, with maximum deviations of +27% and +7%, respectively. When the housing addition is introduced, population of zone 3 rises further while the growth of zone 2 slows slightly, resulting in maxima of +31% for zone 3 and +23% for zone 2. The average population difference in zone 3 increases from +2% in TRAM to +15% in TRAM+HOUSE3, indicating that the housing pulse helps sustain growth above the baseline for a longer period. Conversely, many other zones remain below baseline for much of the combined scenario, showing larger negative average differences and deeper minima. Overall, both TRAM and TRAM+HOUSE3 policy scenarios sustain average population gains in zones 2 and 3, while other zones experience average losses.

Table 10 summarises the change in public transport modal share between zones 2 and 3, compared to the baseline scenario, under the TRAM and TRAM+HOUSE3 policy scenarios. It reports the maximum, average, and standard deviation of changes, over the period following policy implementation (2030–2051). The fast tram increases the public transport modal share between zones 2 and 3, with a larger increase observed for commutes from the central zone 3 to zone 2. To understand this result, the model's causalities are examined. Zone 3, as the central zone with a concentration of jobs, attracts a large number of morning peak commutes, exceeding the flows from zone 3 to zone 2 in the morning. With fewer commuters and lower traffic volume from zone 3 to 2 in the morning, road congestion and car travel times are lower, resulting in a higher share of car commutes from zone 3 to 2 compared to the reverse direction. Consequently, the baseline public transport modal share is lower for trips from zone 3 to 2. With the opening of the fast tram, both zones attract more residents, with zone 3 experiencing a larger surge in absolute population numbers. This leads to a stronger increase in commutes from zone 3 to zone 2, generating greater road congestion in this direction. As a result, the modal shift towards public transport is more pronounced for trips originating from zone 3 under both the TRAM and TRAM+HOUSE3 scenarios. In the TRAM+HOUSE3 case, the shift is even stronger, reflecting the additional population surge in zone 3.

These results highlight that population patterns are dynamic, and that the benefits of infrastructure investments alone may be temporary; coordinated planning of housing and transport is essential to sustain gains and manage unintended outcomes. Moreover, railway and express public transport services, can improve accessibility, reduce vehicle-related pollutants, particulate emissions, and traffic noise, influence land use for potential housing and commercial developments, and support urban regeneration. This underscores the importance of integrated, forward-looking planning.

Table 9: Percentage change in zone populations relative to baseline scenario under (TRAM) and (TRAM+HOUSE3) scenarios for the period 2030-2051.

Scenario / Zone	TRAM			TRAM+HOUSE3		
Zone	**Max**	**Min**	**Average**	**Max**	**Min**	**Average**
1	11%	-16%	-1%	10%	-20%	-5%
2	27%	-11%	4%	23%	-10%	3%
3	7%	-2%	2%	31%	-1%	15%
4	10%	-14%	0%	9%	-17%	-4%
5	13%	-17%	-2%	12%	-23%	-5%
6	10%	-15%	0%	8%	-19%	-4%
7	12%	-15%	0%	10%	-19%	-3%
8	15%	-18%	-2%	14%	-24%	-4%
9	12%	-22%	-3%	14%	-28%	-6%
10	12%	-16%	-1%	10%	-20%	-4%
11	10%	-14%	0%	8%	-17%	-3%
12	13%	-15%	0%	11%	-20%	-3%

Table 10: Change in public transport modal share between zone 2 & 3, compared to baseline scenario under (TRAM) and (TRAM+HOUSE3) scenarios for the period 2030-2051.

Scenario / **Zone**	**TRAM**			**TRAM+HOUSE3**		
	Max	**Average**	**Standard deviation**	**Max**	**Average**	**Standard deviation**
2 to 3	0.13	0.08	0.026	0.12	0.08	0.024
3 to 2	0.17	0.15	0.014	0.22	0.18	0.026

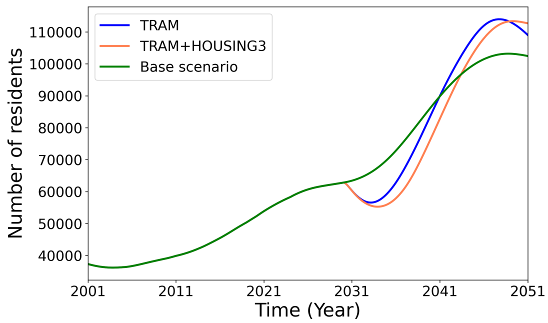

(a) Residents zone 1

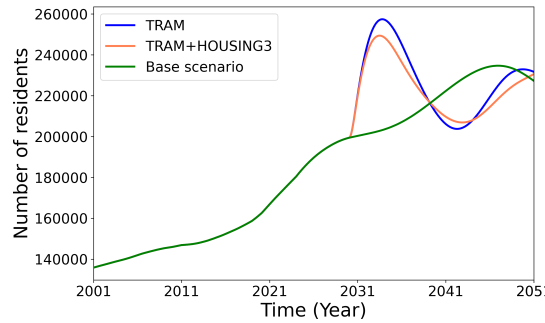

(b) Residents zone 2

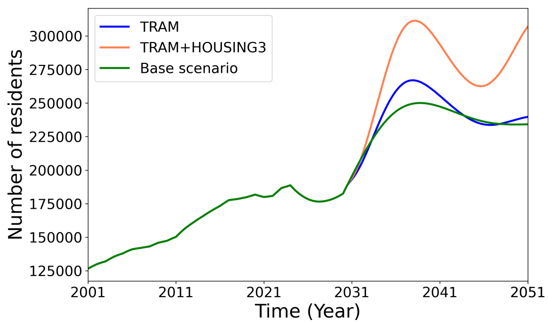

(c) Residents zone 3

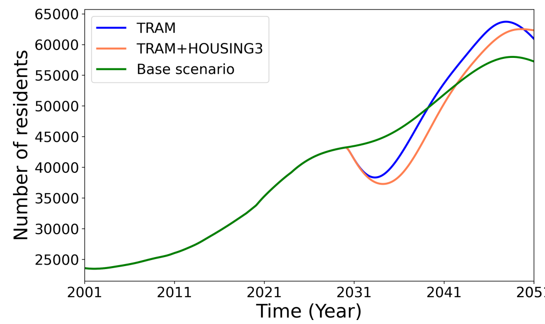

(d) Residents zone 4

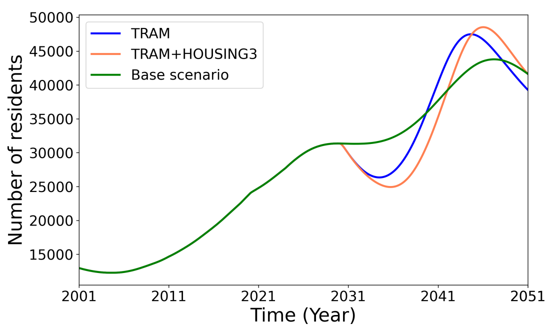

(e) Residents zone 5

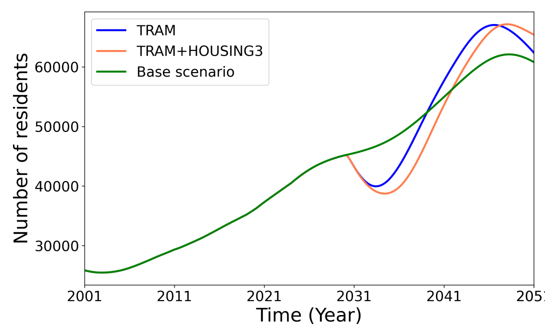

(f) Residents zone 6

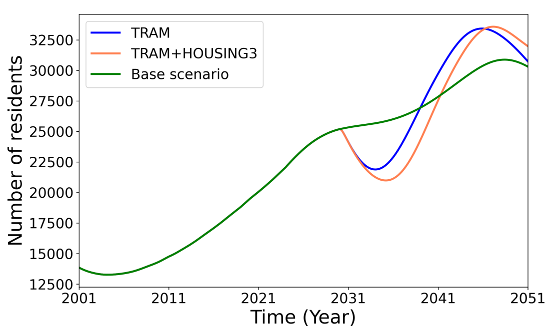

(g) Residents zone 7

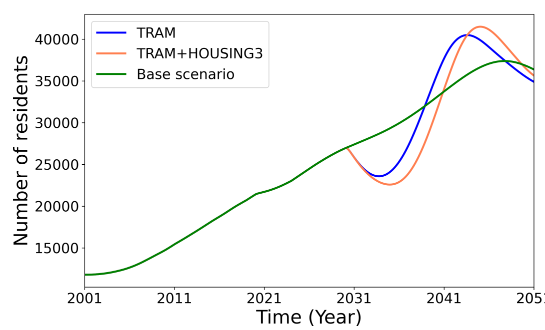

(h) Residents zone 8

Figure 13: Number of residents in each zone under (TRAM) and (TRAM+HOUSE3) scenarios - Continued.

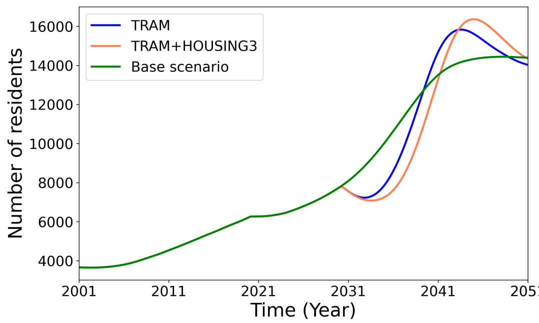

(i) Residents zone 9

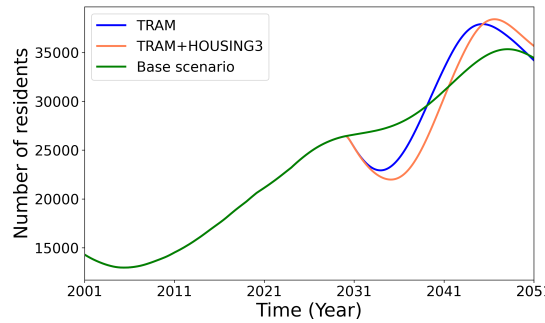

(j) Residents zone 10

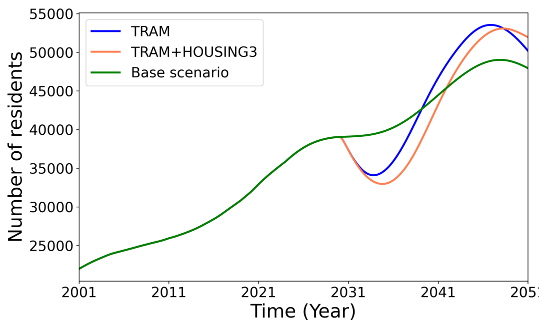

(k) Residents zone 11

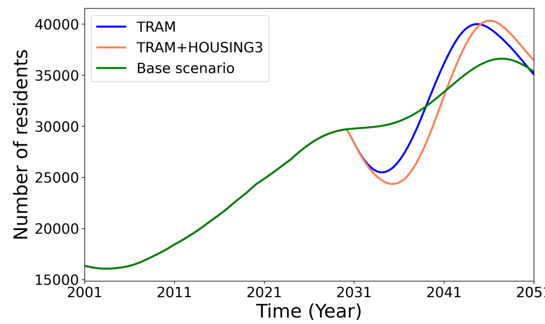

(l) Residents zone 12

Figure 13: Number of residents in each zone under (TRAM) and (TRAM+HOUSE3) scenarios.

6 Conclusion

This study is motivated by having a computational efficient decision support tool that offers a systematic view of combined land use and mobility, aimed at assessing the long-term impacts of transport and land use policies. In this paper, we combine transport and land use models within the same framework, simultaneously considering the development path of the modules over a time period of multiple years with dynamic modelling. The framework explicitly accounts for the interactions and feedback between transport and land use systems. The model is developed based on the principles of System Dynamics, leveraging transport manuals, econometric, and behavioural models for quantification. The choice of system dynamics is motivated by its ability to capture feedback loops and complex nonlinear interactions, represent time delays, and serve as a decision-support tool for assessing long-term policy impacts with high computational efficiency in integrated land use and transport systems.

The framework offers the following key specifications: (i) an integrated design that enables the simultaneous consideration of transport and land use dynamics, (ii) incorporation of transitory equilibrium, with the system state dynamically derived from the model and accommodating different time delays, (iii) daily modelling timesteps, effectively capturing the time delays and reaction speeds of different processes, (iv) representation of the development path over time through dynamic modelling, (v) a modular structure that provides flexibility for incorporating new features and aspects required by the analyst, (vi) reproducible results, (vii) high computational efficiency, (viii) modest data requirements, and (ix) ease of understanding, allowing it to function as a decision-support tool capable of evaluating the combined effects of multiple policies over a time horizon in a manner transparent to decision-makers. The framework also allows the analyst to define the start and end points, as well as the levels, of policy instruments.

Using the framework, a cross-national application is conducted for the Greater Region of Luxembourg. Model parameters are calibrated through a sequential, partly manual process guided by performance metrics to reproduce as closely as possible the observations gathered in the area of study. Calibration is first performed on standalone submodels before integrating them into the full framework, controlling the endless adjustment loop. The model fit and example policy scenarios are analysed. As in most prospective research, the results are not pure predictions but aim to highlight key trends and stimulate debate about possible futures. The findings show that the long-term evolution of population is dynamic, and the benefits of infrastructure investments alone may be temporary without coordinated planning of housing and transport. This underscores the importance of forward-looking strategies with a systematic perspective.

Integrating land use and transport presents multiple challenges and limitations. Data availability and quality are key issues, as models require information from various sources, entities, domains, and spatial scales. In cross-border applications, the coordination of different planning systems add further complexity. Engaging with all relevant stakeholders, harmonising datasets, addressing missing values, and imputing unavailable variables are significant hurdles. Poor data quality can further compromise model accuracy and reliability. Moreover, integration is inherently interdisciplinary, requiring a trans-disciplinary approach to combine expertise from different fields. All models have inherent limitations, yet many can still yield valuable insights. The current integrated framework is no exception. While it is not a universal solution for every urban planning challenge, it offers a powerful lens for examining complex systems, with the flexibility to incorporate additional components and feedback loops as new data becomes available. By recognising and addressing its underlying assumptions, we can leverage the framework's strengths while mitigating its limitations.

The current model has limitations that should be acknowledged. It does not incorporate expectations and assume fully rational or perfect decision-making. Moreover, demographic and economic segmentation—such as age, income, and education groups—is not explicitly represented. Household income, however, can be used as a proxy for neighbourhood quality and incorporated into the residential location choice model. The workplace submodel is assumed exogenous, without capturing endogenous development or relocation of workplaces across zones. Furthermore, the overlap of traffic between different corridors is not considered. Finally, the model does not include a network assignment stage; integrating this functionality would require substantial additional data and resources, a network plan, and an interface to link the model to an external assignment tool. The opportunities for future research are discussed in detail in what follows.

This work offers several avenues for extension and improvement, paving the way for future research. The workplace model is currently assumed to be exogenous; future studies could focus on endogenising workplace relocation dynamics by incorporating employment location choice into the framework. Additional dimensions of choice complexity could also be explored. For example, while renting is currently the sole means to meet housing needs, incorporating the option of buying would provide a more comprehensive representation of residential demand, enabling a detailed analysis of the interplay between renting and buying decisions. Moreover, incorporating the evolution of the population's age structure and analysing household transitions such as children leaving home, household separation, and couple formation would enrich the model's demographic realism. Expanding the framework to include education and income groups, and studying their evolution over time under various policy scenarios presents another valuable research direction. Different population segments have distinct preferences and place varying importance on specific attributes and variables in their decision-making. Rather than assuming homogeneous preferences across the entire population, segmenting the population and analysing their characteristics in residential and transport choices would enhance the model's capacity to capture heterogeneity (Schultheiss et al., 2024; Escolano-Utrilla et al., 2024). The current model specifications are deterministic. Introducing stochasticity and exploring probabilistic formulations could capture uncertainty more realistically and enhance the robustness of the model's outcomes.

The framework can also be extended to incorporate additional transport mode choices, including soft modes such as cycling and walking, enabling more comprehensive analyses of modal shares. Further enhancements could involve integrating variables such as distance to public transport stops, frequency of public transport services, and latent factors like perceived convenience of car and public transport. Moreover, parking availability and pricing play a critical role in mode choice; incorporating parameters such as parking capacity, pricing, and average time spent searching for parking would represent a valuable extension of the model. Two factors that may change significantly over the considered time horizon are car ownership and technological developments, such as improvements in fuel consumption, electric mobility, and autonomous vehicles. These require further investigation and present interesting directions for model extension. In addition, emerging services such as shared mobility could have substantial impacts and should be considered in future modelling efforts. Currently, car ownership is not included in the model specifications; incorporating it into travel mode choice models could enhance their realism. In addition, the changing attitudes and preferences of the population over the modelling horizon are aspects that warrant further study and should be considered in future work.

Moreover, a wider spectrum of accessibility indicators can be considered and tested within the framework, with the choice guided by specific policy questions and evaluation criteria (van Wee, 2015). Further work may also investigate alternative definitions of accessibility, integrating subjective dimensions such as perceived travel time quality alongside traditional measures of cost and time. In addition, causal discovery algorithms could be applied to extract and validate causal structures from observed data. Applying such methods to model location and transportation choices, as demonstrated in recent studies that combine causal discovery with structural equation modelling (Chauhan et al., 2024), could strengthen the framework's capacity to identify and interpret underlying causal relationships.

With richer data on cross-border regions, the model's simplifications for cross-national zones can be relaxed. For example, in the case study of the Greater Region of Luxembourg, access to data from the Luxmobil survey (Ministere du Developpment durable et des Infrastructures, 2017), which contains representative information on the travel behaviour of both cross-border commuters and residents, would allow for more detailed modelling. Assumptions regarding cross-border zones, such as the distribution of cross-border trips across Luxembourg's internal cantons, could be refined.

One important policy under consideration is the promotion of remote work arrangements, such as work-from-home and satellite offices near borders, to reduce commute times for cross-border commuters. Studying the societal (e.g., inequalities between residents and cross-border workers due to tax and social security hurdles), spatial (impacts on daily mobility, land use, and air pollution), and economic (effects on productivity) implications of teleworking is essential for understanding how people perceive remote work and its broader effects. This would enable a more comprehensive perspective on how telework can transform mobility and land use patterns. For example, the survey data collected in the ongoing WinWin4WorkLife project (WinWin4WorkLife Consortium, 2025) can provide valuable insights into perceptions of telework and its influence on location choice and mobility behaviour. Additionally, examining how telework affects workplace relocation would add complexity to the analysis of its impact on daily travel and residential preferences. Investigating the spatial-temporal rebound effects of telework, such as the fragmentation of activities and changes in travel patterns, represents another promising research avenue. Such analysis would help policymakers and practitioners better anticipate potential unintended consequences of telework, facilitating more effective urban planning and promoting sustainable city development (Ratnasari and Van Acker, 2024).

The calibration of integrated transport and land use models remains an important research challenge (Kii et al., 2019). Typically, calibration is performed by an expert modeller who iteratively adjusts a set of parameters to match observed data from the study area as closely as possible. This process is often conducted manually, with minimal automation, requiring repeated parameter adjustments. Exploring non-manual calibration methods capable of simultaneously adjusting multiple parameters, along with developing robust estimation procedures, could significantly advance these integrated models. However, the data-intensive nature of disaggregate estimation approaches should be carefully considered when pursuing such developments. Additionally, the risk of over-parameterisation and overfitting warrants attention. Implementing a model selection scheme that balances model complexity with goodness of fit can help mitigate these risks and improve the likelihood of achieving accurate and reliable predictions (Capelle et al., 2019).

Creating harmonised databases that combine transport, demographic, and land use information, and supplementing these with cross-border travel surveys, would significantly strengthen integrated studies at cross-national scales. For instance, the MMUST+ project (*Modèle multimodal et scénarios de mobilité transfrontalier (MMUST+)*, 2025), collects cross-border travel data that provides valuable insights into the links between residential patterns and daily mobility. Furthermore, improving the effectiveness of modelling and predictive tools requires a deeper understanding of the factors that could encourage behavioural change. Stated preference surveys can provide behaviourally credible insights into how individuals might adjust their mobility patterns in response to new service offerings, infrastructure developments, or modifications to existing systems. Finally, future research could compare model results with more disaggregate formulations to evaluate the extent to which greater detail may alter aggregated outcomes and policy implications.

Acknowledgments

We would like to thank the team at the Luxembourg Institute of Socio-Economic Research (LISER), specially Antoine Paccoud, Frédéric Docquier, and Philippe Gerber for data acquisition and project initiative.

References

Acheampong, R. A. and Silva, E. A. (2015). Land use–transport interaction modeling: A review of the literature and future research directions, *J. Transp. Land Use* **8**(3): 11–38. DOI: 10.5198/jtlu.2015.806.

Administration du Cadastre et de la Topographie (n.d.). Limites administratives du Grand-Duché de Luxembourg.

Aljoufie, M., Zuidgeest, M., Brussel, M., van Vliet, J. and van Maarseveen, M. (2013). A cellular automata-based land use and transport interaction model applied to Jeddah, Saudi Arabia, *Landsc. Urban Plan.* **112**(1): 89–99. DOI: 10.1016/j.landurbplan.2013.01.003.

Alonso, W. (1964). *Location and land use: Toward a general theory of land rent*, Harvard university press, Cambridge, U.K. DOI: 10.4159/harvard.9780674730854.c8.

Anas, A. (1994). METROSIM: A unified economic model of transportation and land-use, *Williamsville, NY Alex Anas Assoc.* .

Anas, A. and Liu, Y. (2007). A regional economy, land use, and transportation model (RELU-TRAN©): Formulation, algorithm design, and testing, *J. Reg. Sci.* **47**(3): 415–455. DOI: 10.1111/j.1467-9787.2007.00515.x.

Axhausen, K., Horni, A. and Nagel, K. (2016). *The Multi-Agent Transport Simulation MATSim*, Ubiquity Press. DOI: 10.5334/baw.

Baraklianos, I., Bouzouina, L., Bonnel, P. and Aissaoui, H. (2020). Does the accessibility measure influence the results of residential location choice modelling?, *Transportation (Amst).* **47**(3): 1147–1176. DOI: 10.1007/s11116-018-9964-6.

Barlas, Y. (1996). Formal aspects of model validity and validation in system dynamics, *Syst. Dyn. Rev.* **12**(3): 183–210. DOI: 10.1002/(sici)1099-1727(199623)12:3<183::aid-sdr103>3.0.co;2-4.

Batty, M. (1971). Modelling cities as dynamic systems, *Nature* **231**: 425–428.

Ben-Akiva, M. and Bowman, J. L. (1998). Integration of an activity-based model system and a residential location model, *Urban Stud.* **35**(7): 1131–1153. DOI: 10.1080/0042098984529.

Bhat, C. R. and Guo, J. Y. (2007). A comprehensive analysis of built environment characteristics on household residential choice and auto ownership levels, *Transp. Res. Part B Methodol.* **41**(5): 506–526. DOI: 10.1016/j.trb.2005.12.005.

Bierlaire, M., de Palma, A., Hurtubia, R. and Waddell, P. (2015). *Integrated transport and land use modeling for sustainable cities*, EPFL Press, Lausanne, Switzerland.

Black, J. (2018). *Urban Transport Planning*, Routledge, London.

Bravo, M., Briceño, L., Cominetti, R., Cortés, C. E. and Martínez, F. (2010). An integrated behavioral model of the land-use and transport systems with network congestion and location externalities, *Transp. Res. Part B Methodol.* **44**(4): 584–596. DOI: 10.1016/j.trb.2009.08.002.

California Department of Transportation (2022). Cal-B / C Parameter Guide, *Technical report*, California Department of Transportation.

Capelle, T., Sturm, P., Vidard, A. and Morton, B. J. (2019). Calibration of the Tranus land use module: Optimisation-based algorithms, their validation, and parameter selection by statistical model selection, *Comput. Environ. Urban Syst.* **77**: 101146. DOI: 10.1016/j.compenvurbsys.2017.04.009.

Chang, J. S. and Mackett, R. L. (2006). A bi-level model of the relationship between transport and residential location, *Transp. Res. Part B Methodol.* **40**(2): 123–146. DOI: 10.1016/j.trb.2005.02.002.

Chauhan, R. S., Riis, C., Adhikari, S., Derrible, S., Zheleva, E., Choudhury, C. F. and Pereira, F. C. (2024). Determining causality in travel mode choice, *Travel Behav. Soc.* **36**(100789). DOI: 10.1016/j.tbs.2024.100789.

Chen, H., Chen, B., Zhang, L. and Li, H. X. (2021). Vulnerability modeling, assessment, and improvement in urban metro systems: A probabilistic system dynamics approach, *Sustain. Cities Soc.* **75**: 103329. DOI: 10.1016/j.scs.2021.103329.

Coppola, P. and Nuzzolo, A. (2011). Changing accessibility, dwelling price and the spatial distribution of socio-economic activities, *Res. Transp. Econ.* **31**(1): 63–71. DOI: 10.1016/j.retrec.2010.11.009.

Dautel, V., Docquier, F., Paccoud, A. and Verheyden, B. (2024). The economic Impact of cross-border workers in Luxembourg: Labor market dynamics, housing market developments, and technological externalities.

de la Barra, T. (1989). *Integrated land use and transport modelling: Decision chains and hierarchies*, Cambridge University Press, Cambridge, UK:. DOI: 10.1016/0191-2607(90)90039-9.

de Palma, A., Motamedi, K., Picard, N. and Waddell, P. (2005). A model of residential location choice with endogenous housing prices and traffic for the Paris region, *Eur. Transp. / Trasp. Eur.* **31**: 67–82.

Department for transport, directorate for mobility planning (2018). Modu 2.0 - Sustainable Mobility Strategy, *Technical report*, Department of Transport, Directorate for Mobility Planning Based.

Domencich, T. A. and McFadden, D. (1975). *Urban travel demand: A behavioral analysis*.

Echeñique, M., Crowther, D. and Lindsay, W. K. (1969). A spatial model of urban stock and activity, *Reg. Stud.* **3**: 281–312.

Echenique, M. H., Flowerdew, A. D., Hunt, J. D., Mayo, T. R., Skidmore, I. J. and Simmonds, D. C. (1990). The Meplan models of bilbao, Leeds and Dortmund: Foreign summaries, *Transp. Rev.* **10**(4): 309–322. DOI: 10.1080/01441649008716764.

Escolano-Utrilla, S., López-Escolano, C. and Salvador-Oliván, J. A. (2024). Size and spatial and functional structure of aggregate daily mobility networks in functional urban areas: Integrating adjacent spaces at several scales, *Cities* **145**(104731). DOI: 10.1016/j.cities.2023.104731.

Fabolude, G., Knoble, C., Vu, A. and Yu, D. (2025). Smart cities, smart systems: A comprehensive review of system dynamics model applications in urban studies in the big data era, *Geogr. Sustain.* **6**(1): 100246. DOI: 10.1016/j.geosus.2024.10.002.

Feldman, O. and Simmonds, D. (2005). Land-use modelling with DELTA: Update and experience, *Proc. Ninth Int. Conf. Comput. Urban Plan. Urban Manag.*

Fontoura, W. B., Chaves, G. d. L. D. and Ribeiro, G. M. (2019). The Brazilian urban mobility policy: The impact in São Paulo transport system using system dynamics, *Transp. Policy* **73**(April 2017): 51–61. DOI: 10.1016/j.tranpol.2018.09.014.

Forrester, J. W. (1961). *Industrial Dynamics*, MIT Press, Cambridge, Massachusetts.

Forrester, J. W. (1970). Urban dynamics, *Ind. Manag. Rev.* **11**(3).

Gerber, P., Caruso, G., Cornelis, E. and Médard de Chardon, C. (2018). A multi-scale fine-grained luti model to simulate land-use scenarios in Luxembourg, *J. Transp. Land Use* **11**(1): 255–272. DOI: 10.5198/jtlu.2018.1187.

Goldner, W. (1971). The Lowry model heritage, *J. Am. Plan. Assoc.* **37**(2): 100–110. DOI: 10.1080/01944367108977364.

Haghani, A., Sang, Y. L. and Joon, H. B. (2003a). A system dynamics approach to land use transportation system performance modeling, Part 1: Methodology, *J. Adv. Transp.* **37**(1): 1–82.

Haghani, A., Sang, Y. L. and Joon, H. B. (2003b). A system dynamics approach to land use transportation system performance modeling, Part 2: Application, *J. Adv. Transp.* **37**(1): 1–82.

Haque, M. B., Choudhury, C., Hess, S. and dit Sourd, R. C. (2019). Modelling residential mobility decision and its impact on car ownership and travel mode, *Travel Behav. Soc.* **17**: 104–119. DOI: 10.1016/j.tbs.2019.07.005.

Hyman, G. (1969). The calibration of trip distribution models, *Environ. Plan.* **1**(1): 105–112. DOI: 10.1068/a010105.

Ibeas, Á., Cordera, R., Dell'Olio, L. and Coppola, P. (2013). Modelling the spatial interactions between workplace and residential location, *Transp. Res. Part A Policy Pract.* **49**: 110–122. DOI: 10.1016/j.tra.2013.01.008.

International Energy Agency (2021). Fuel economy in the European Union, *Technical report*, International Energy Agency.

Johansen, B. G., Hansen, W. and Tennoy, A. (2015). Evaluation of models and methods for analyzing the interaction between land-use , infrastructure and traffic demand in urban areas, *Technical report*, Institute of Transport Economics Norwegian Centre for Transport Research.

Kaufmann, V. and Jemelin, C. (2003). Coordination of land-use planning and transportation: How much room to manoeuvre?, *Int. Soc. Sci. J.* **55**(176): 295–305. DOI: 10.1111/j.1468-2451.2003.05502009.x.

Khosravi, S., Haghshenas, H. and Salehi, V. (2020). Macro-Scale Evaluation of Urban Transportation Demand Management Policies in CBD by Using System Dynamics Case Study: Isfahan CBD, *Transp. Res. Procedia* **48**(2018): 2671–2689. DOI: 10.1016/j.trpro.2020.08.246.

Kii, M., Moeckel, R. and Thill, J. C. (2019). Land use, transport, and environment interactions: WCTR 2016 contributions and future research directions, *Comput. Environ. Urban Syst.* **77**: 101335. DOI: 10.1016/j.compenvurbsys.2019.04.002.

Lau, K. H. and Kam, B. H. (2005). A cellular automata model for urban land-use simulation, *Environ. Plan. B Plan. Des.* **32**(2): 247–263. DOI: 10.1068/b31110.

Le, H., Gurry, F. and Lennox, J. (2023). An application of land use, transport, and economy interaction model, *Res. Transp. Econ.* **99**: 101294. DOI: 10.1016/j.retrec.2023.101294.

Lee, B. H. and Waddell, P. (2010). Residential mobility and location choice: A nested logit model with sampling of alternatives, *Transportation (Amst).* **37**(4): 587–601. DOI: 10.1007/s11116-010-9270-4.

Lennox, J. (2023). Spatial economic dynamics in transport project appraisal, *Econ. Model.* **127**(August): 106464. DOI: 10.1016/j.econmod.2023.106464.

Lerman, S. (1976). Location, housing, automobile ownership, and mode to work: a joint choice mode, *Transp. Res. Rec.* pp. 6–11.

Lopane, F. D., Kalantzi, E., Milton, R. and Batty, M. (2023). A land-use transport-interaction framework for large scale strategic urban modeling, *Comput. Environ. Urban Syst.* **104**. DOI: 10.1016/j.compenvurbsys.2023.102007.

Lowry, I. (1964). A model of metropolis, *Technical report*, Santa Monica Rand Corporation, Santa Monica, CA.

Mackett, R. (1983). The Leeds integrated land-use transport model (LILT), *Technical report*, Institute for Transport Studies, University of Leeds, Leeds, UK.

Markus Maibach, Peter;, M. and Sutter, D. (2006). Analysis of operating cost in the EU and the US. Annex 1 to COMPETE Final Report, *Technical report*, European Commission, Karlsruhe, Germany.

Martínez, F. J. and Henríquez, R. (2007). A random bidding and supply land use equilibrium model, *Transp. Res. Part B Methodol.* **41**(6): 632–651. DOI: 10.1016/j.trb.2006.08.003.

McFadden, D. (1974). The measurement of urban travel demand, *J. Public Econ.* **3**(4): 303–328. DOI: 10.1016/0047-2727(74)90003-6.

Miller, E. J. (2020). Measuring Accessibility: Methods & Issues, *Int. Transp. Forum Discuss. Pap.*

Ministère de l'Aménagement du Territoire (2023). Programme directeur d'amenagement du territoire (PDAT), *Technical report*, le Gouvernement du Grand-Duché de Luxembourg, Luxembourg.

Ministere du Developpment durable et des Infrastructures (2017). Luxmobil 2017: Enquête sur la mobilité des résidents au Luxembourg, *Technical report*, Département de la mobilité et des transport.

Ministry of Housing and Spatial Planning (2025). Housing Observatory.

Ministry of Mobility and Public Works (MMTP), Department of Mobility and Transport, D. o. M. P. (2022). *PNM 2035 - National Mobility Plan*, Ministry of Mobility and Public Works Department of Mobility and Transport Directorate of Mobility Planning.

MMUST (2022). Grande enquête de mobilité - Résultats des préférences révélées, *Technical report*, Projet MMUST (Modéliser les Mobilités Urbaines et Sociales Transfrontalières).

Mobilitéit (2025). Public transport of Luxembourg. DOI: https://www.mobiliteit.lu/en/tickets-page/national-tickets/.

Modèle multimodal et scénarios de mobilité transfrontalier (MMUST+) (2025).

Moeckel, R., Chou, A. T., Garcia, C. L. and Okrah, M. B. (2018). Trends in integrated land-use/transport modeling: An evaluation of the state of the art, *J. Transp. Land Use* **11**(1): 463–476. DOI: 10.5198/jtlu.2018.1205.

Moeckel, R., Schwarze, B., Spiekermann, K. and Wegener, M. (2007). Simulating interactions between land use, transport and environment, *Proc. 11th World Conf. Transp. Res.*, Berkeley, CA: University of California at Berkeley.

Mokhtarian, P. L. and Cao, X. (2008). Examining the impacts of residential self-selection on travel behavior: A focus on methodologies, *Transp. Res. Part B Methodol.* **42**(3): 204–228. DOI: 10.1016/j.trb.2007.07.006.

Niedzielski, M. A. and Eric Boschmann, E. (2014). Travel time and distance as relative accessibility in the journey to work, *Ann. Assoc. Am. Geogr.* **104**(6): 1156–1182. DOI: 10.1080/00045608.2014.958398.

Observatoire du développement territorial (2025). L'emploi des acifs occupés au Luxembourg, *Technical Report 3*, Ministère du Logement et de l'Aménagement du territoire.

Odysse Muree (2024). Sectoral Profile - Transport, *Technical report*.

Ortuzar, J. d. D. and Willumsen, L. G. (2011). *Modelling Transport*, 4 edn, Wiley, Chichester, UK.

Pfaffenbichler, P. (2003). *The strategic, dynamic and integrated urban land use and transport model MARS (Metropolitan Activity Relocation Simulator)*, PhD thesis, TU Wien.

Pfaffenbichler, P., Emberger, G. and Shepherd, S. (2008). The integrated dynamic land use and transport model MARS, *Networks Spat. Econ.* **8**(2-3): 183–200. DOI: 10.1007/s11067-007-9050-7.

Pfaffenbichler, P., Harrison, G., Shepherd, S., Gühnemann, A., Jittrapirom, P. and Gomez Vilchez, J. (2024). In the loop: The application of system dynamics in transport, *Transp. Res. Arena*, Dublin, Ireland. DOI: 10.5281/zenodo.11056813.

Pinjari, A. R., Bhat, C. R. and Hensher, D. A. (2009). Residential self-selection effects in an activity time-use behavior model, *Transp. Res. Part B Methodol.* **43**(7): 729–748. DOI: 10.1016/j.trb.2009.02.002.

Pinto, N., Antunes, A. P. and Roca, J. (2021). A cellular automata model for integrated simulation of land use and transport interactions, *ISPRS Int. J. Geo-Information* **10**(3). DOI: 10.3390/ijgi10030149.

Putman, S. H. (1983). Integrated urban models, *Policy Anal. Transp. L. use* **10**.

Ratnasari, A. F. and Van Acker, V. (2024). TELECITY - Investigating rebound effects of telework and its implications on cities.

Rhinocarhire.com (2025). Fuel prices in Luxembourg.

RTL Today (2023a). Speed limit soon reduced to 90km/h during rush hour?

RTL Today (2023b). When is peak rush hour in Luxembourg City?

Salvini, P. and Miller, E. J. (2005). ILUTE: An operational prototype of a comprehensive microsimulation model of urban systems, *Networks Spat. Econ. 5(2)* **5**(2): 217–234.

Schultheiss, M. E., Pattaroni, L. and Kaufmann, V. (2024). Planning urban proximities: An empirical analysis of how residential preferences conflict with the urban morphologies and residential practices, *Cities* **152**(105215). DOI: 10.1016/j.cities.2024.105215.

Shen, Q., Chen, Q., sin Tang, B., Yeung, S., Hu, Y. and Cheung, G. (2009). A system dynamics model for the sustainable land use planning and development, *Habitat Int.* **33**(1): 15–25. DOI: 10.1016/j.habitatint.2008.02.004.

Shepherd, S. P. (2014). A review of system dynamics models applied in transportation, *Transp. B* **2**(2): 83–105. DOI: 10.1080/21680566.2014.916236.

Simmonds, D. (2016). Transport modelling, microsimulation and other issues in land-use/economic/transport modelling practice., *Symp. Integr. Land-Use Transp. Model.*, Raitenhaslach, Germany.

Simmonds, D. C. (1999). The Delta land use modeling package, *Environ. Plan. B Plan. Des.* **26**: 665–684.

Simmonds, D., Waddell, P. and Wegener, M. (2013). Equilibrium versus dynamics in urban modelling, *Environ. Plan. B Plan. Des.* **40**(6): 1051–1070. DOI: 10.1068/b38208.

Sivakumar, A. (2007). Modelling transport: A Synthesis of transport modelling methodologies, *Technical report*, Imperial College of London.

Statec (2017). Projections macroéconomiques et démographiques de long terme: 2017-2060, *Technical report*, Institut national de la statistique et et des études économiques (STATEC).

Statista Research Department (2025). Luxembourg: Monthly unleaded gasoline prices.

Sterman, J. D. (2000). *Systems thinking and modeling for a complex world*, Irwin McGraw-Hill, Boston, Boston: McGraw-Hill.

Swanson, J. and Gleave, S. D. (2008). Transport and the urban economy: The urban dynamic model J, *Innovation* **2**: 28–32.

Timmermans, H. (2006). Modelling land use and transportation dynamics: Methodological issues, state-of-art, and applications in developing countries, *Technical report*, Urban Planning Group, Eindhoven University of Technology, The Netherlands.

Tscharaktschiew, S. and Hirte, G. (2012). Should subsidies to urban passenger transport be increased? A spatial CGE analysis for a German metropolitan area, *Transp. Res. Part A Policy Pract.* **46**(2): 285–309. DOI: 10.1016/j.tra.2011.09.006.

Ummah, M. S. (2019). Organizing e-mobility in cities - chances and risks, *Sustain.* **11**(1): 1–14.

van Wee, B. (2015). Toward a new generation of land use transport interaction models, *J. Transp. Land Use* **8**(3): 1–10.

Vega, A. and Reynolds-Feighan, A. (2009). A methodological framework for the study of residential location and travel-to-work mode choice under central and suburban employment destination patterns, *Transp. Res. Part A Policy Pract.* **43**(4): 401–419. DOI: 10.1016/j.tra.2008.11.011.

Ventana Systems (2025). Vensim Personal Learning Edition (PLE).

Ville de Luxembourg (2025). Affordable housing.

Von Neumann, J. (1968). The general and logical theory of automata, *Syst. Res. Behav. Sci.*, Cambridge: MIT Press.

Waddell, P. (2002). Urbansim: Modeling urban development for land use, transportation, and environmental planning, *J. Am. Plan. Assoc.* **68**(3): 297–314. DOI: 10.1080/01944360208976274.

Waddell, P. (2014). Integrated land use and transportation planning and modelling: Addressing challenges in research and practice, *Transp. Model. Urban Plan. Pract.*, Routledge, p. 22.

Walczak, A. and Mathae, T. (2018). Statistics on cross-border workers in the greater region, *Technical report*.

Walker, R. and Wakeland, W. (2011). Calibration of complex system dynamics models: A practioner's report, *Technical report*.

Wegener, M. (2021). Land-use transport interaction models, *Handb. Reg. Sci.*, Springer, Berlin, Heidelberg.

White, M. J. (1988). Location choice and commuting behavior in cities with decentralized employment, *J. Urban Econ.* **24**(2): 129–152. DOI: 10.1016/0094-1190(88)90035-6.

Wikipedia contributors (2025). Transport in Luxembourg.

WinWin4WorkLife Consortium (2025). WinWin4WorkLife.

Xie, Y. and Batty, M. (2004). Integrated urban evolutionary modeling, *GeoDynamics* **44**(0): 273–294. DOI: 10.1201/9781420038101-24.

Yang, L., Zheng, G. and Zhu, X. (2013). Cross-nested logit model for the joint choice of residential location, travel mode, and departure time, *Habitat Int.* **38**: 157–166. DOI: 10.1016/j.habitatint.2012.06.002.

Yu, Y., He, J., Tang, W. and Li, C. (2018). Modeling Urban collaborative growth dynamics using a multiscale simulation model for theWuhan urban agglomeration area, China, *ISPRS Int. J. Geo-Information* **7**(5): 1–13. DOI: 10.3390/ijgi7050176.

Zhang, Z. and Li, J. (2022). Spatial suitability and multi-scenarios for land use: Simulation and policy insights from the production-living-ecological perspective, *Land use policy* **119**: 106219. DOI: 10.1016/j.landusepol.2022.106219.

Zhao, L. and Peng, Z. R. (2012). LandSys: An agent-based Cellular Automata model of land use change developed for transportation analysis, *J. Transp. Geogr.* **25**: 35–49. DOI: 10.1016/j.jtrangeo.2012.07.006.